Journal of Medicinal Chemistry

Article

Discovery of Novel Pazopanib-based HDAC and VEGFR Dual Inhibitors Targeting Cancer Epigenetics and Angiogenesis Simultaneously

Jie Zang, Xuewu Liang, Yongxue Huang, Yuping Jia,
Xiaoyang Li, Wenfang Xu, C. James Chou, and Yingjie Zhang

J. Med. Chem., **Just Accepted Manuscript** • DOI: 10.1021/acs.jmedchem.8b00384 • Publication Date (Web): 22 May 2018

ACS Publications

is published by the American Chemical Society. 1155 Sixteenth Street N.W., Washington, DC 20036

Discovery of Novel Pazopanib-based HDAC and VEGFR Dual Inhibitors Targeting Cancer Epigenetics and Angiogenesis Simultaneously

Jie Zang[†], Xuewu Liang[†], Yongxue Huang[‡], Yuping Jia[§], Xiaoyang Li[‖], Wenfang Xu[†], C. James Chou[‖] and Yingjie Zhang[†,*]

[†]Department of Medicinal Chemistry, School of Pharmaceutical of Science, Shandong University, Ji'nan, Shandong, 250012, PR China

[‡]Weifang Bochuang International Biological Medicinal Institute, Weifang, Shandong, 261061, PR China

[§]Shandong Academy of Pharmaceutical Sciences, Ji'nan, Shandong, 250101, PR China

[‖]Department of Drug Discovery and Biomedical Sciences, South Carolina College of Pharmacy, Medical University of South Carolina, Charleston, SC, 29425, United States

ABSTRACT: Herein a novel series of pazopanib hybrids as polypharmacological antitumor agents were developed based on the crosstalk between histone deacetylases (HDACs) and vascular endothelial growth factor (VEGF) pathway. Among them, one *ortho*-aminoanilide **6d** and one hydroxamic acid **13f** exhibited considerable total HDACs and VEGFR-2 inhibitory activities. The HDAC inhibitory activities endowed **6d** and **13f** with potent antiproliferative activities, which was not observed in the approved VEGFR inhibitor pazopanib. Compounds **6d** and **13f** possessed comparable HDAC isoform selectivity profiles to the clinical class I HDAC inhibitor MS-275 and the approved pan-HDAC inhibitor SAHA, respectively. **6d** and **13f** also exhibited uncompromised multiple tyrosine kinases inhibitory activities relative to pazopanib. The intracellular dual inhibition to HDAC and VEGFR of **6d** and **13f** was validated by western blot analysis. In both HUVECs tube formation assay and rat thoracic aorta rings assay, **6d** and **13f** showed comparable antiangiogenic potencies to pazopanib. What's more, **6d** possessed desirable pharmacokinetic profiles with the oral bioavailability of 72% in SD rats and considerable *in vivo* antitumor efficacy in a human colorectal adenocarcinoma (HT-29) xenograft

model.

INTRODUCTION

Mechanism-based drugs targeting a specific biological molecule or pathway is one of the major breakthroughs in cancer therapy in the past several decades.[1] However, the clinical effectiveness of such single target drugs is generally transitory, being followed by almost-inevitable resistance and relapses due to the adaptive nature and heterogeneity of tumor cells and tumor microenvironment.[2, 3] The limitations of single target drugs can be overcome by multiple target drugs, which not only can attack multiple hallmark capabilities of cancer simultaneously to get more robust and durable therapeutic effects, but also can avoid the risks involved in multicomponent drug cocktails, such as unpredictable pharmacokinetic profiles, drug−drug interactions and poor patient compliance.[4-7]

Both genetic and epigenetic aberrations contribute to tumorigenesis and development. Compared with genetic aberrations, epigenetic aberrations are more druggable due to its reversibility regulated by various enzymes.[8, 9] Among the numerous epigenetic enzymes, histone deacetylases (HDACs) are a family of important therapeutic targets for cancer, inflammation, neurological disorders and infections.[10, 11] Thus far, four HDAC inhibitors, vorinostat (SAHA), romidepsin (FK228), belinostat (PXD101) and panobinostat (LBH589) were approved by the US Food and Drug Administration (FDA), and one HDAC inhibitor chidamide (CS005) was approved by the China Food and Drug Administration (CFDA) for the treatment of hematologic cancer (Figure 1)[12]. Despite the efficacy in hematologic malignancies, HDAC inhibitor and other epigenetic agents have not shown significant efficacy as monotherapy against solid tumors. Inspiringly, combination therapies offer hope to conquer this challenge.[13-16] In addition, considering the above-mentioned advantages compared with combination therapy,[4-7] intense interest is drawn to the discovery of HDAC inhibitor-based multitarget antitumor agents.[17-22]

Angiogenesis, one key physiology of solid tumors required for tumor growth and metastasis, has long been recognized as a target for cancer therapy.[23, 24] Among the various angiogenic factors, vascular endothelial growth factor (VEGF)/vascular endothelial growth factor receptor (VEGFR) signaling pathway is considered as the primary antiangiogenesis target, with over ten monoclonal antibodies and small molecular inhibitors approved for the treatment of solid tumors.[25-27] Pazopanib (Figure 1), a multiple VEGFR inhibitor,[28] has already been approved by the FDA for the treatment of advanced renal cell carcinoma and advanced soft tissue sarcoma in 2009 and 2012, respectively.[29] A phase II study indicated that second-line treatment with pazopanib in relapsed and refractory small-cell lung cancer (SCLC) was well tolerated and resulted in promising objective responses and disease control.[30] However, drug resistance and tumor relapse occurred in nearly all patients treated with pazopanib and other VEGFR inhibitors.[31-33] To overcome the drug resistance and enhance the antitumor efficacy, combination therapies using pazopanib and diverse HDAC inhibitors were carried out and showed encouraging preclinical *in vitro* and *in vivo* results.[34-36] Notably, the results of a phase I clinical study supported further evaluation of the combination of pazopanib and HDAC inhibitor SAHA in cancer patients with mutated *TP53*, especially in those with metastatic sarcoma or metastatic colorectal cancer.[37] Another phase I clinical study of pazopanib plus HDAC inhibitor abexinostat (Figure 1) showed that epigenetic modification with HDAC inhibition could enhance response and reverse resistance to pazopanib in patients with renal cell carcinoma and other solid tumor malignancies.[38] This study also showed that the clinical benefit was significantly correlated with both peripheral blood mononuclear cell (PBMC) HDAC2 expression and fold change in PBMC histone H4 acetylation, supporting HDAC2 as the clinically relevant target to restore and enhance response to VEGF-targeting therapy.[38]

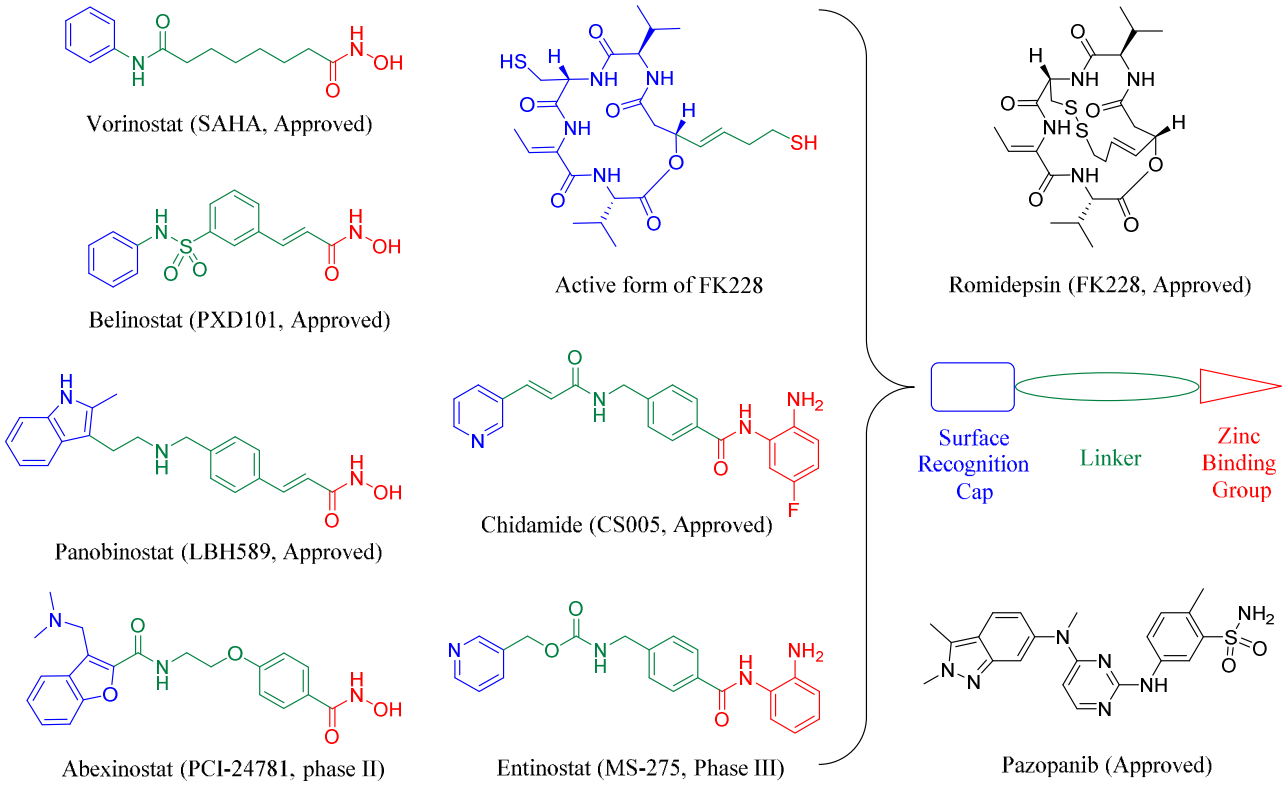

Figure 1. The structures of several representative HDAC inhibitors and one VEGFR inhibitor pazopanib. The three parts of HDAC inhibitor pharmacophore model are indicated in three different colors, respectively.

Herein, based on the prevalent strategy of multitarget drug and the clinical benefit of HDAC inhibitor and VEGFR inhibitor combination, a novel series of pazopanib-based HDAC and VEGFR dual inhibitors were rationally designed and readily synthesized. Comprehensive evaluation identified compound **6d** with simultaneous HDAC/VEGFR inhibitory activity, potent *in vitro* antiproliferative and antiangiogenic potency, desirable *in vivo* pharmacokinetic profiles and antitumor efficacy.

RESULTS AND DISCUSSION

Rational Design of Novel HDAC and VEGFR Dual Inhibitors Derived from Pazopanib. Most HDAC inhibitors share a general pharmacophore (Figure 1) composed of a zinc binding group that chelates the catalytic zinc ion, a hydrophobic linker that occupies the tunnel of the active site, and a surface recognition cap that interacts with the amino acid residues around the entrance of the active

site.[39] Considering the surface recognition cap can tolerate extraordinarily variable structures, even like the cyclic depsipeptide in FK228, we believed that incorporation of pazopanib into the surface recognition cap of HDAC inhibitor pharmacophore could obtain dual inhibitors of HDAC and VEGFR. To determine which site of pazopanib can be modified without compromising its VEGFR inhibitory activity, the proposed binding mode of pazopanib in the ATP pocket of VEGFR-2 was analyzed using our in-house molecular docking study (Figure 2A). We could see that the indazole moiety of pazopanib fit well into the inside pocket of VEGFR-2, and the 2-aminopyrimidine moiety formed two important hydrogen binds with Cys917 in the hinge region. Therefore, modification of these two moieties could not be well tolerated. Note that the benzenesulfonamide moiety was projected towards the solvent region, where could be installed with HDAC inhibitor module while minimally interfering the binding with VEGFR. Based on these analysis, two privileged zinc binding groups (hydroxamic acid and *ortho*-aminoanilide) were attached to the solvent-exposed phenyl group of pazopanib directly or via various linkers, leading to the structurally diverse pazopanib-based HDAC and VEGFR dual inhibitors (Figure 2B).

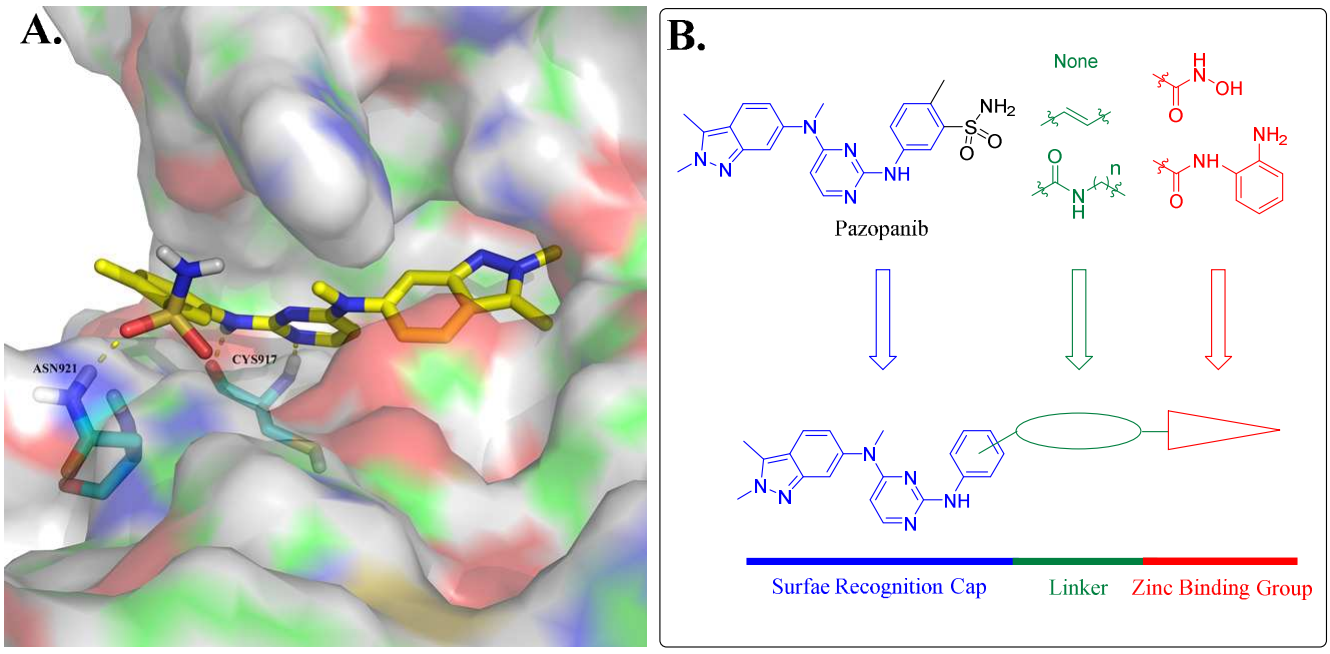

Figure 2. A. The proposed binding mode of pazopanib in the ATP pocket of VEGFR-2 (PDB code: 3CJG). The figure was generated using PyMol (http://www.pymol.org/); **B.** The design strategy of Pazopanib-based HDAC and VEGFR dual inhibitors. Note that the delimitation of the surface recognition cap and the linker is variable dependent on the linker length.

Chemistry. The procedures to synthesize the target compounds **6a-6e** were outlined in Scheme 1. Commercially available 2,3-Dimethyl-2*H*-indazol-6-amine (**1**) as the starting material reacted with 2, 4-dichloropyrimidine to afford **2**, which was treated with CH_3I to obtain **3**. Then compound **3** was treated with 4-aminobenzoic acid, 3-aminobenzoic acid and 5-amino-2-methylbenzoic acid to produce the key intermediates **4a-4c**, respectively. Reaction of **4a-4c** with $SOCl_2$ in methanol afforded **5a-5c**, which were directly converted into hydroxamic acids **6a-6c** by NH_2OK in dry methanol. In addition, the intermediate **4a** and **4b** could react with 1,2-diaminobenzene by TBTU-mediated amide formation to afford *ortho*-aminoanilides **6d** and **6e**, respectively.

Scheme 1. **Synthesis of Compounds 6a-6e**[a]

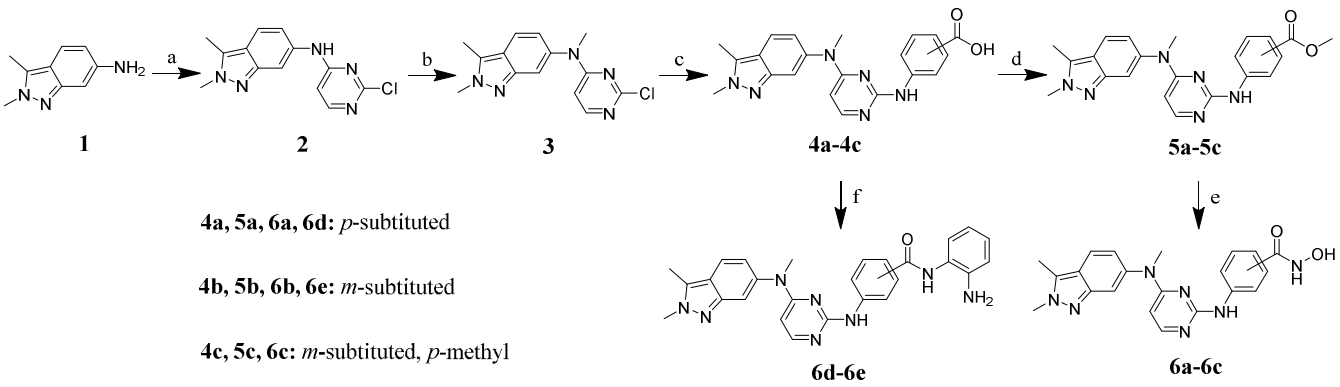

[a]Reagents and conditions: (a) 2,4-dichloropyrimidine, $NaHCO_3$, EtOH, reflux, 4 h, 90%; (b) CH_3I, Cs_2CO_3, DMF, rt, 2 h, 80%; (c) various aminobenzoic acids, isopropanol, conc. HCl, reflux, 4 h, 79-90%; (d) $SOCl_2$, CH_3OH, reflux, 4 h, 93-95%; (e) $NH_2OH.HCl$, KOH, anhydrous CH_3OH, rt, 2 h, 40-57%; (f) 1,2-diaminobenzene, TBTU, TEA, anhydrous DMF, ice bath, 30 min, rt, 12 h, 43-65%;

Target compounds **10a** and **10b** were synthesized using the procedures described in Scheme 2. The intermediate **4a** and **4b** were treated with *N, O*-dimethylhydroxylamine hydrochloride to give Weinreb amides **7a** and **7b**, which were then reduced via $LiAlH_4$ to afford aldehydes **8a** and **8b**, respectively. The Horner-Wadsworth-Emmons reaction of **8a** and **8b** with triethyl phosphonoacetate led to **9a** and **9b,** which were directly converted into hydroxamic acids **10a** and **10b** by NH_2OK in dry methanol, respectively.

Scheme 2. **Synthesis of Compounds 10a-10b**[a]

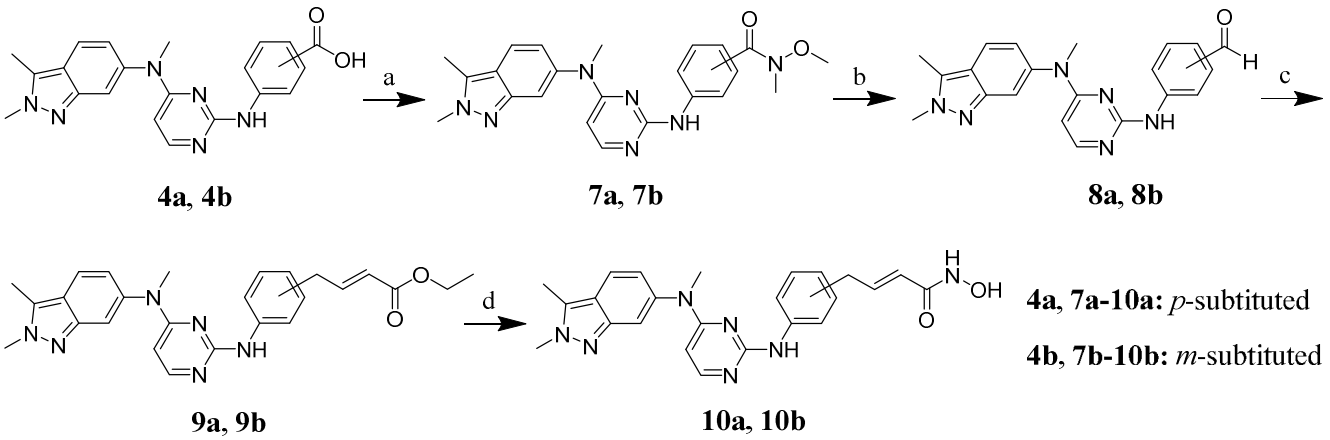

[a]Reagents and conditions: (a) *N*,*O*-dimethylhydroxylamine hydrochloride, TBTU, TEA, anhydrous DMF, ice bath, 30 min, rt, 12 h, 71-72%; (b) $LiAlH_4$, anhydrous THF, -40 °C, 4 h, 70-72%; (c) triethyl phosphonoacetate, NaH, anhydrous THF, ice bath, 20 min, rt, 12 h, 65-68%; (d) $NH_2OH.HCl$, KOH, anhydrous CH_3OH, rt, 2 h, 60-64%.

The procedures to prepare the target compounds **13a-13i** and **14a-14g** were outlined in scheme 3. The intermediates **4a-4c** were coupled with various methyl aminoalkanoates to get compounds **11a-11i**, which could be transformed to hydroxamic acids **13a-13i**, respectively. Besides, hydrolysis of compounds **11a-11g**, followed by condensation with 1,2-diaminobenzene led to *ortho*-aminoanilide **14a-14g**, respectively.

Scheme 3. **Synthesis of Compounds 13a-13i and 14a-14g**[a]

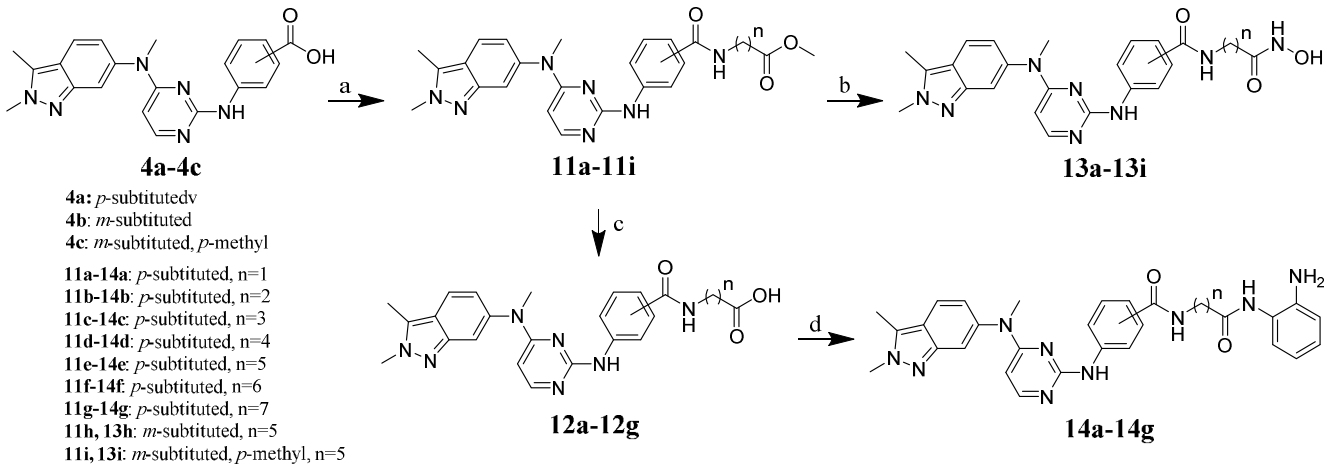

[a]Reagents and conditions: (a) various methyl aminoalkanoates, TBTU, TEA, anhydrous DMF, ice bath, 30 min, rt, 12 h, 69-80%; (b) $NH_2OH.HCl$, KOH, anhydrous CH_3OH, rt, 2 h, 51-61%; (c) 3M NaOH, CH_3OH, rt, 4 h, 81-90%; (d) 1,2-diaminobenzene, TBTU, TEA, anhydrous DMF, ice bath, 30 min, rt, 12 h, 38-48%.

In Vitro HDAC and VEGFR Inhibition Assay. To minimally alter the structure of pazopanib, two zinc binding groups, hydroxamic acid and *ortho*-aminoanilide, were directly attached to the *para*- or *meta*-position of the solvent-exposed phenyl group of pazopanib, leading to compounds **6a-6e**. The HDAC inhibitory activities of **6a-6e** were evaluated by determining the IC_{50} values against HeLa nuclear extract, with the hydroxamic acid-based compound SAHA and *ortho*-aminoanilide-based compound MS-275 as positive controls. Their VEGFR inhibitory activities were preliminarily tested by determining the VEGFR-2 inhibitory rates at 200 nM with pazopanib as the positive control. Results in Table 1 showed that all hydroxamic acids (**6a-6c**) displayed much less potent HDAC inhibitory activities than the positive control SAHA, probably because the short linkers of **6a-6c** could not lead their hydroxamate groups to the zinc ion. Note the *para*-substituted **6a** exhibited better HDAC and VEGFR-2 inhibitory activities than the *meta*-substituted **6b** and **6c**. For *ortho*-aminoanilide analogs (**6d** and **6e**), *para*-substituted **6d** showed more potent HDAC and VEGFR-2 inhibitory activities than *meta*-

substituted compound **6e**, which was in accordance with the trend in hydroxamates. Importantly, compound **6d** not only exhibited comparable HDAC inhibitory activity to MS-275, but also exhibited comparable VEGFR-2 inhibitory activity to pazopanib, validating our compound design strategy that incorporation of zinc binding group to the solvent-exposed phenyl group of pazopanib could obtain HDAC and VEGFR dual inhibitors. To get dual inhibitors with improved HDAC inhibitory activity, compounds **10a** and **10b** with *N*-hydroxycinnamamide fragment were designed and synthesized. *N*-hydroxycinnamamide is a privileged structure used by many potent HDAC inhibitors including the approved drug LBH589 and PXD101. Enzyme inhibition results (Table 1) showed that compared with **6a** and **6b**, **10a** and **10b** exhibited dramatically increased HDAC activities and uncompromised VEGFR-2 activities, indicating that introduction of longer linker was benefit to HDAC inhibition and not detrimental to VEGFR inhibition. However, **10a** and **10b** were still over 10-fold less potent than SAHA.

Table 1. Structure and In Vitro Enzymatic Inhibition of 6a-6e and 10a-10b

Compd	Structures	HDAC IC_{50} (μM)[a]	VEGFR-2 inhibition rate at 0.2 μM
6a	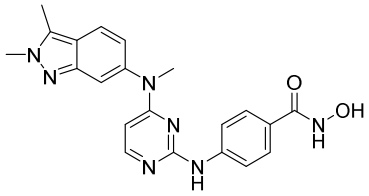	11.3	99%
6b	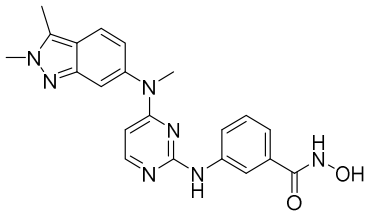	>20	77%

6c	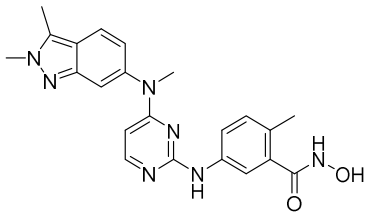	>20	74%
6d	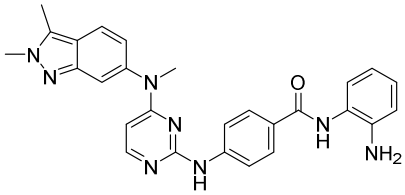	4.6	100%
6e	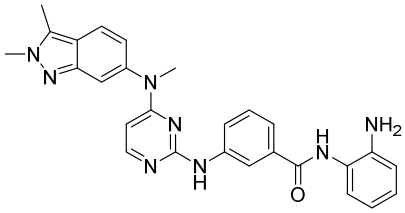	21.3	63%
10a	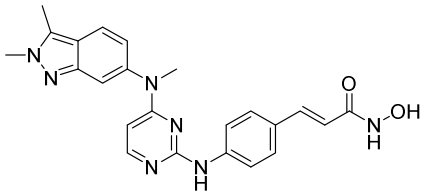	1.4	95%
10b	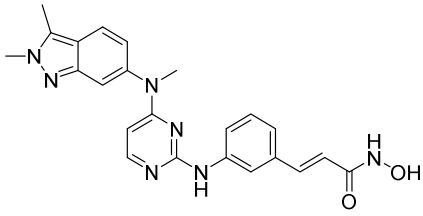	3.0	97%
SAHA	-	0.13	ND[b]
MS275	-	1.8	ND[b]
Pazopanib	-	ND[b]	95%

[a]Assays were performed in replicate (n≥2); the SD value are <20% of the mean.

[b]Not determined.

To further investigate the effects of linker on HDAC and VEGFR inhibition, hydroxamic acid-based compounds **13a-13i** and *ortho*-aminoanilide-based compounds **14a-14g** were designed and synthesized. Their enzyme inhibition results were shown in Table 2. For *para*-substituted hydroxamic acids **13a-**

13g, their HDAC inhibitory activities first increased and then decreased with the linker length, culminating in compound **13f** (n = 6), which was about 40-fold more potent than SAHA. Such structure-activity relationship was also found in *ortho*-aminoanilides **14a-14g**, among which compound **14e** with the optimal linker length (n = 5) exhibited comparable HDAC inhibitory activity to MS-275. Similar with the results in Table 1, *meta*-substituted hydroxamic acids **13h** and **13i** also exhibited inferior HDAC inhibition compared with their *para*-substituted analog **13e**. Interestingly, neither the linker length nor the substituted position had significant influence on VEGFR-2 inhibition of these dual inhibitors.

Table 2. Structure and In Vitro Enzymatic Inhibition of 13a-13i and 14a-14g

Compd	Structures	HDAC IC_{50} (μM)[a]	VEGFR-2 inhibition rate at 0.2 μM
13a	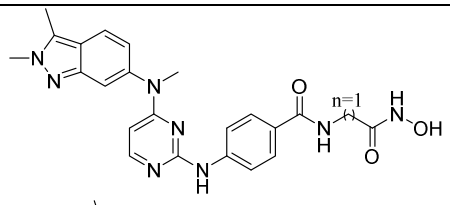	>20	95%
13b	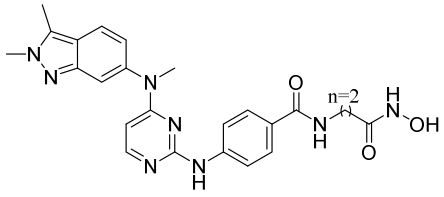	>20	99%
13c	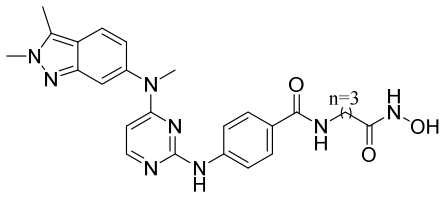	19.8	99%
13d	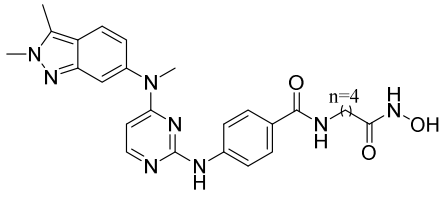	0.68	94%

13e	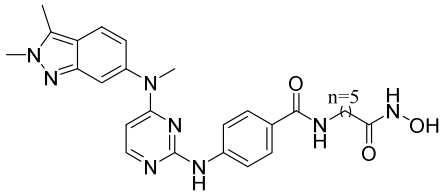	0.017	98%
13f	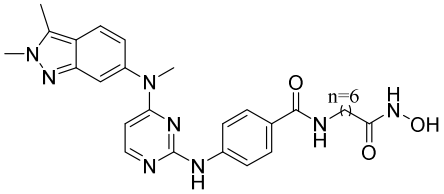	0.0033	93%
13g	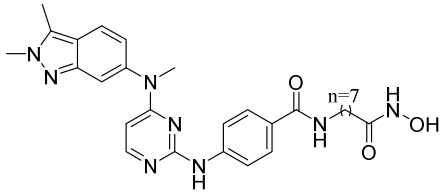	0.025	92%
13h	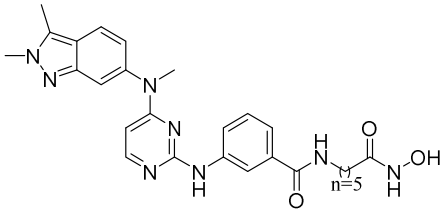	0.18	90%
13i	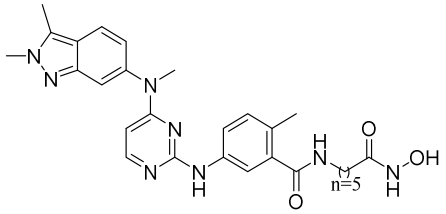	0.82	87%
14a	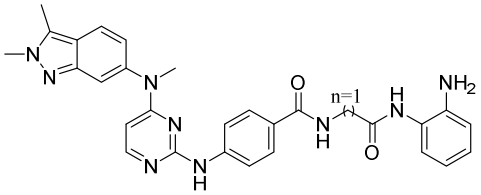	>20	98%
14b	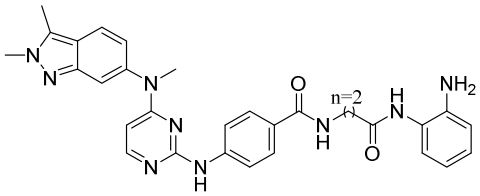	>20	97%
14c	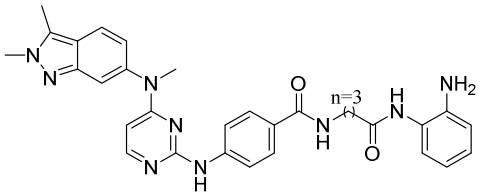	19.0	96%

14d	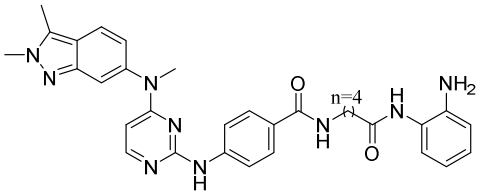	15.1	94%
14e	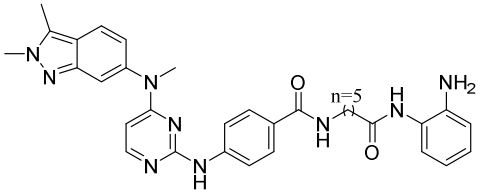	3.0	95%
14f	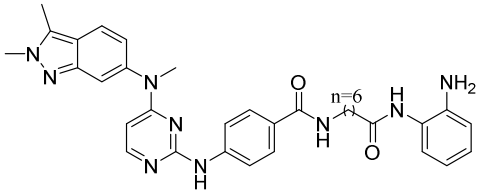	5.0	93%
14g	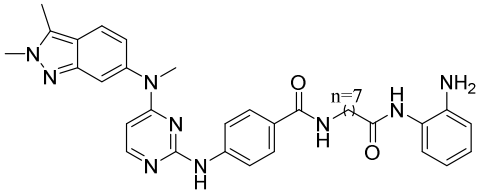	8.7	92%
SAHA	-	0.13	ND[b]
MS275	-	1.8	ND[b]
Pazopanib	-	ND[b]	95%

[a]Assays were performed in replicate (n≥2); the SD value are <20% of the mean.

[b]Not determined

In Vitro Antiproliferation Assay. Considering their potent HDAC inhibitory potencies, four hydroxamic acids (**10a**, **13e**, **13f**, **13g**) and four *ortho*-aminoanilides (**6d**, **14e**, **14f**, **14g**) were evaluated for their antiproliferative activities against seven solid tumor cell lines and four hematological tumor cell lines. According to the results in Table 3, all the HDAC and VEGFR dual inhibitors showed moderate to potent activities, while the VEGFR inhibitor pazopanib was not active, demonstrating that the HDAC inhibitory activities of these dual inhibitors contributed to their antiproliferative capacities. Generally, our compounds and the two positive controls SAHA and MS-275 were more potent against the hematological tumor cell lines over the solid tumor cell lines. However, because the main purpose

of our research was to find dual inhibitors for solid tumor therapy, we focused our attention on identifying target compounds with potent activities against solid tumor cell lines. Among the tested solid tumor cell lines, the human colorectal adenocarcinoma cell line HT-29 seemed to be the most sensitive one to our compounds. It was worth noting that the *ortho*-aminoanilide-based compound **6d** exhibited more potent antiproliferative activity against HT-29 than both SAHA and MS-275. Besides, though less potent than SAHA in HT-29, the hydroxamic acid-based compound **13f** was slightly more potent than MS-275. The cytotoxicities of **13f** and **6d** against normal cells were determined using human umbilical vein endothelial cells (HUVECs). It was revealed that the IC_{50} values of **13f** and **6d** against HUVECs were 21.1 μM and 16.0 μM, respectively, much higher than their IC_{50} values against tumor cell lines. Note that **13f** and **6d** showed lower or comparable cytotoxicities against HUVECs than pazopanib plus HDAC inhibitors (SAHA or MS275), despite their higher cytotoxicities relative to pazopanib, SAHA or MS275 alone (Table S1 in Supporting Information).

Table 3. In Vitro Growth-Inhibitory Activities of Selected Compounds

Compd	IC_{50} (μM)[a]										
	solid tumor cell lines							hematological tumor cell lines			
	HT-29	ACHN	AGS	HeLa	PC-3	MDA-MB-231	HT-1080	KG1	HEL	MOLT-4	K562
10a	2.96	3.85	>5	4.93	1.60	2.59	3.25	1.02	0.75	0.59	1.66
13e	ND[b]	ND[b]	ND[b]	ND[b]	>5	ND[b]	>5	2.31	2.56	0.60	2.89
13f	2.51	>5	4.44	4.36	1.69	2.96	1.97	1.60	2.80	0.31	0.99
13g	ND[b]	ND[b]	ND[b]	ND[b]	3.42	ND[b]	>5	0.93	1.04	0.27	1.10
SAHA	1.51	2.08	4.23	2.06	>5	3.02	2.54	1.52	0.19	0.36	1.52
6d	1.07	>5	>5	1.71	2.38	3.74	>5	0.67	1.52	0.94	1.82
14e	ND[b]	ND[b]	ND[b]	ND[b]	>5	ND[b]	ND[b]	3.15	2.06	0.87	4.31
14f	ND[b]	ND[b]	ND[b]	ND[b]	>5	ND[b]	ND[b]	3.14	1.16	1.15	4.15
14g	2.96	3.62	>5	3.07	>5	2.57	>5	2.68	0.49	0.56	3.97
MS275	3.10	2.40	0.34	>5	>5	2.55	>5	>5	0.44	0.45	3.66
Pazo	>5	>5	>5	>5	>5	>5	>5	>5	>5	>5	>5

Pazo represents Pazopanib

[a]Assays were performed in replicate (n≥2); the SD value are <20% of the mean.

[b]Not determinded

HDAC and Kinase Selectivity Profile. In general, hydroxamic acid-based HDAC inhibitors show little discrimination among different Zn^{2+}-dependent HDACs (class I, class II and class IV), while *ortho*-aminoanilide-based HDAC inhibitors are selective for class I. Therefore, to profile the selectivity of these HDAC and VEGFR dual inhibitors, two representative hydroxamic acids **10a** and **13f** were tested against two class I isoforms (HDAC2/8) and one class II isoform (HDAC6) with SAHA as positive control, two representative *ortho*-aminoanilides **6d** and **14g** were tested against three class I isoforms (HDAC1/2/3) with MS-275 as positive control. The results in Table 4 indicated that compared with SAHA, compound **13f** possessed comparable HDAC2/6 inhibitory activities, and much better HDAC8 inhibition. It also revealed that compound **6d** and MS-275 exhibited almost equivalent inhibition towards HDAC1/2/3.

Table 4. HDACs Isoform Selectivity Profile of Representative Compounds

Compd	IC_{50} (μM)[a]				
	HDAC1	HDAC2	HDAC3	HDAC6	HDAC8
10a	ND[b]	5.30	ND[b]	1.03	2.89
13f	ND[b]	0.38	ND[b]	0.072	1.66
SAHA	ND[b]	0.22	ND[b]	0.091	>5
6d	0.59	0.91	0.43	ND[b]	ND[b]
14g	1.46	1.26	0.66	ND[b]	ND[b]
MS275	0.16	0.40	0.61	ND[b]	ND[b]

[a]Assays were performed in replicate (n≥2); the SD value are <20% of the mean.

[b]Not determinded

Based on the considerable HDAC inhibitory and antiproliferative activities of **6d** and **13f**, their VEGFR-2 IC_{50} values were determined and compared with pazopanib (Table 5). Satisfyingly, both **6d** (IC_{50} = 37 nM) and **13f** (IC_{50} = 46 nM) exhibited uncompromised VEGFR-2 inhibitory activities relative to pazopanib (IC_{50} = 34 nM), which was in line with our preliminary VEGFR-2 inhibition results shown in Table 1 and Table 2. Moreover, compounds **6d** and **13f** were evaluated against several other kinases including VEGFR-1, VEGFR-3, PDGFRβ, FGFR1, C-Fms and C-Kit. We chose these tyrosine receptor kinases for the reason that they are all tumor-related targets inhibited by pazopanib.[28] Strikingly, **6d** and **13f** could potently inhibit all the tested kinases with IC_{50} values at the same range of pazopanib (Table 5). Note that **6d** was more potent than **13f** and was even equivalent to pazopanib, probably because compared with **13f**, the structure of **6d** was more similar to that of pazopanib. These results provided solid evidence that rational structural modification of the solvent-exposed phenyl group of pazopanib was well tolerated for its kinase inhibition profile.

Table 5. Kinase Selectivity Profile of Representative Compounds

Compd	IC_{50} (μM)[a]						
	VEGFR-2	VEGFR-1	VEGFR-3	PDGFRβ	FGFR1	C-Fms	C-Kit
6d	0.037	0.022	0.046	0.088	0.192	0.351	0.125
13f	0.046	0.035	0.113	0.111	0.409	0.581	0.163
Pazopanib	0.034	0.098	0.046	0.083	0.163	0.274	0.118

[a]Assays were performed in replicate (n≥2); the SD value are <20% of the mean.

Molecular Docking Study. The proposed binding modes of **6d** and **13f** in the ATP binding pocket of VEGFR-2 were analyzed using Sybyl X_2.1. As we expected, the attached HDAC functional groups of **6d** (Figure 3A) and **13f** (Figure 3B) were projected towards the solvent region. Comparison of **6d** and **13f** with pazopanib revealed that their indazole and 2-aminopyrimidine moieties were superimposed

pretty well. Just like pazopanib, the 2-aminopyrimidine moiety of **6d** and **13f** could also form two hydrogen bonds with Cys917 in the hinge region. For pazopanib, another hydrogen bond between the sulfamide group and Asn921 was observed. In the case of **6d**, a similar hydrogen bond was formed between Asn921 and the amide group. Though **13f** could not form hydrogen bond with Asn921, two extra hydrogen bonds with Glu848 were formed via its hydroxamic acid group. These results rationalized the potent VEGFR-2 inhibitory activities of **6d** and **13f**.

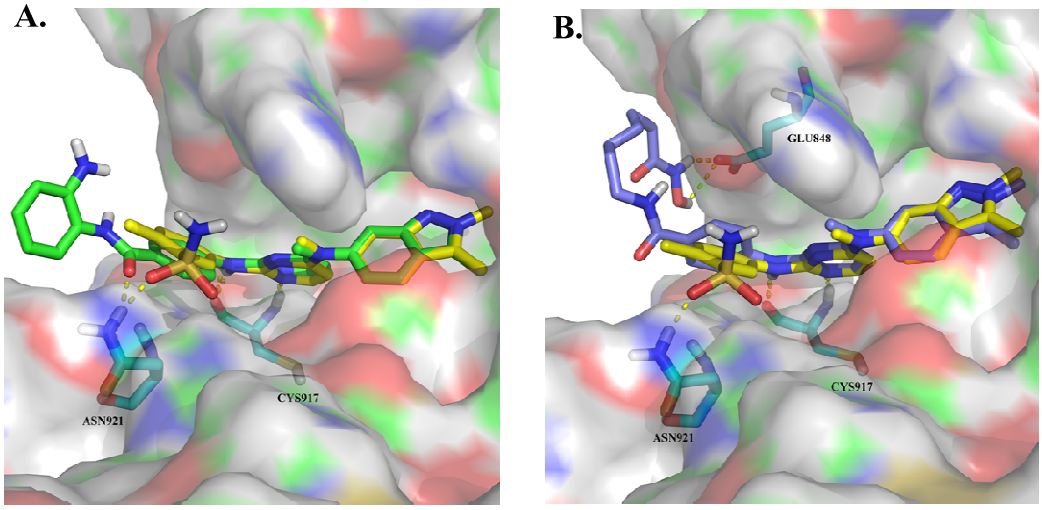

Figure 3. **A.** Overlap of the proposed binding modes of compounds **6d** (green) and pazopanib (yellow) in VEGFR-2 (PDB code: 3CJG); **B.** Overlap of the proposed binding modes of compounds **13f** (purple) and pazopanib (yellow) in VEGFR-2 (PDB code: 3CJG). Yellow dashed lines represent the hydrogen bonds. Oxygen, nitrogen and polar hydrogen atoms are shown in red, blue and white, respectively. The figure was generated using PyMol (http://www.pymol.org/).

The binding modes of **6d** and **13f** in relevant HDAC isoforms proposed by molecular docking study also supported their considerable HDAC inhibitory activities. Figure 4A showed the overlap of **6d** and MS-275 in the active site of HDAC2. We could see that the *N*-(2-aminophenyl)benzamide moieties of **13f** and MS-275 were well superimposed, forming multiple key interactions with HDAC2, such as

chelation with Zn^{2+}, hydrogen bonds with Asp161 and Gly154, and face-to-face π-π stacking with Phe155. The overlaps of **13f** and SAHA in HDAC2 (Figure 4B) and HDAC6 (Figure 4C) displayed the classical binding mode of aliphatic hydroxamic acids: the hydroxamic acid groups chelate the Zn^{2+} in a bidentate manner and form multiple hydrogen bonds, the aliphatic chains occupy the hydrophobic channel, and the aromatic terminal groups interact with the amino acid residues around the entrance of the active site.

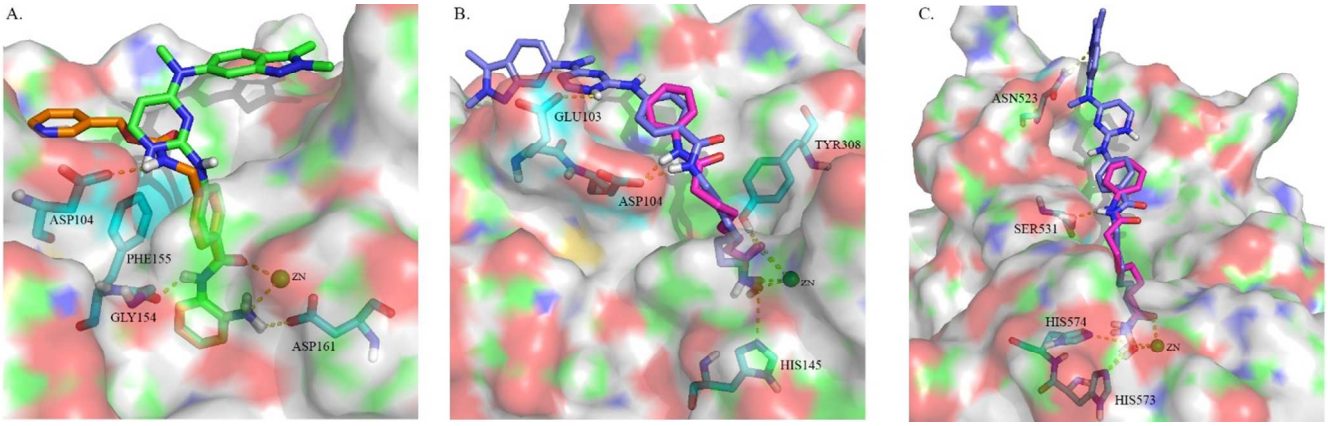

Figure 4. **A.** Overlap of the proposed binding modes of compounds **6d** (green) and **MS275** (orange) in HDAC2 (PDB code: 5IWG). **B.** Overlap of the proposed binding modes of compounds **13f** (purple) and SAHA (magenta) in HDAC2 (PDB code: 5IWG); **C.** Overlap of the proposed binding modes of compounds **13f** (purple) and SAHA (magenta) in HDAC6 (PDB code: 5EEI). Yellow dashed lines indicate the hydrogen bonds or metal interactions. Oxygen, nitrogen and polar hydrogen atoms are shown in red, blue and white, respectively. The figure was generated using PyMol (http://www.pymol.org/).

Western Blot Analysis. Western blot analysis was conducted to confirm the intracellular efficacies of **6d** and **13f**. Results in Figure 5A showed that compound **6d** (1μM) could significantly increase the intracellular levels of the HDAC1/2/3 substrate acetyl-histone H4 (Ac-HH4), which was comparable, if not better than that of MS-275 at the same concentration. Neither **6d** nor MS-275 had significant

influence on the levels of the HDAC6 substrate acetyl-tubulin (Ac-Tub), confirming the class I HDAC selectivity of these *ortho*-aminoanilides. In contrast, the hydroxamic acid **13f** (100 nM) could simultaneously increase the levels of Ac-HH4 and Ac-Tub. At the same concentration, the intracellular efficacies of **13f** on Ac-HH4 and Ac-Tub were inferior to and superior to those of SAHA, respectively, which were in line with their enzyme inhibition results shown in Table 4 that **13f** possessed inferior HDAC2 inhibitory activity but superior HDAC6 inhibitory activity relative to SAHA. In addition, 100 nM of **6d**, **13f** and pazopanib could completely inhibit the phosphorylation of VEGFR-2 in HUVECs (Figure 5B), verifying their potent VEGFR-2 inhibitory activities in cellular context. However, HDAC inhibitors SAHA and MS-275 had no influence on phosphorylation of VEGFR-2.

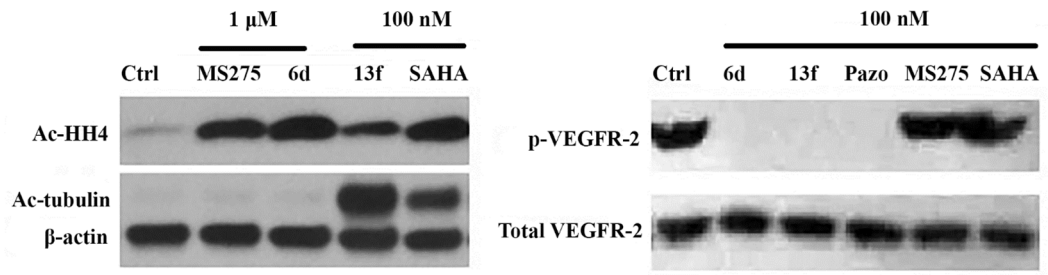

Figure 5. **A.** HeLa cells were treated with DMSO or compounds for 6 h. The levels of acetyl-tubulin (Ac-Tub) and acetyl-histone H4 (Ac-HH4) were determined by immunoblotting. β-Actin was used as a loading control. **B.** HUVEC cells were treated with DMSO or compounds for 2 h, then stimulated with VEGF (50 ng/ml). The levels of phosphorylated VEGFR-2 (p-VEGFR-2) were determined by immunoblotting. Total VEGFR-2 was used as a loading control. Pazo represents pazopanib.

In Vitro HUVECs Tube Formation Assay. Encouraged by their remarkable VEGFR inhibitory activities, compounds **6d** and **13f** were progressed to *in vitro* HUVECs tube formation assay to evaluate their anti-angiogenesis potencies. To avoid the cytotoxicities of tested compounds, HUVECs were treated with compounds at the low concentration of 100 nM. Results in Figure 6 showed that **6d** and

13f could inhibit the tube formation as effectively as pazopanib.

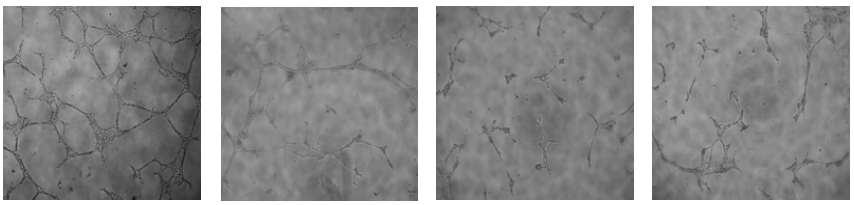

Ctrl **Pazopanib** (0.1 μM) **6d** (0.1 μM) **13f** (0.1 μM)

Figure 6. Representative images of the capillary-like tubular network of HUVECs treated with DMSO or compounds.

Ex Vivo Rat Thoracic Aorta Rings (TARs) Assay. Compared with HUVECs tuber formation model, rat thoracic aorta rings (TARs) assay could better simulate the in vivo angiogenic environment and condition. Therefore, we performed ex vivo rat TARs assay to further evaluate the antiangiogenic activity of **6d** and **13f**. As clearly presented in Figure 7, in the negative control group, a mass of microvessels sprouted from the thoracic aorta ring. In contrast, compounds **6d** and **13f** as well as the positive control pazopanib, dramatically inhibited the microvessel outgrowth.

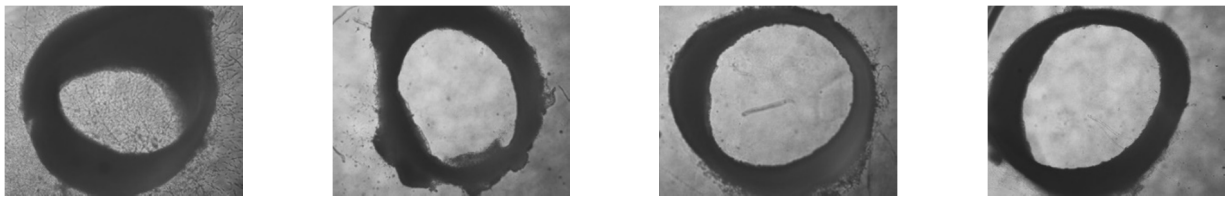

Ctrl **Pazopanib** (5 μM) **6d** (5 μM) **13f** (5 μM)

Figure 7. Representative images of rat thoracic aorta rings treated with DMSO or compounds.

In Vivo Pharmacokinetic (PK) Profile. Though the in vitro activities of **6d** and **13f** were comparable, only **6d** was progressed to in vivo pharmacokinetic study because of the potential metabolic liability of hydroxamic acid-based compounds.[40] The hydrochlorate of **6d** was administrated intravenously (IV) at 2 mg/kg or orally (PO) at 10 mg/kg in Sprague−Dawley (SD) rats. The concentration–time curves and PK parameters of **6d** were respectively shown in Figure 8 and Table 6, which indicated the desirable PK properties of **6d** (hydrochlorate). Importantly, **6d** (hydrochlorate)

possessed the high oral bioavailability (F) of 72 %, warranting further evaluation of its oral antitumor activity.

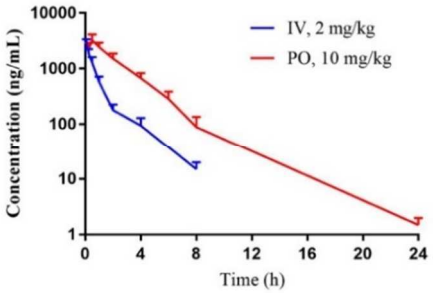

Figure 8. The concentration–time curves of **6d** in SD rats following IV (2 mg/kg) or PO (10 mg/kg) administration.

Table 6. PK Parameters of 6d in SD Rats (N = 6)

Dose (mg/kg)	Route	$t_{1/2}$ (h)	T_{max} (h)	C_{max} (ng/mL)	AUC_{0-t} (ng*h/mL)	MRT_{0-t} (h)	Vz (mL/kg)	CL (mL/h/kg)	F (%)
2	IV	1.64	0.08	2775	2377	1.13	2061	876	
10	PO	2.10	0.5	3245	8571	2.54			72

In Vivo Antitumor Activity Evaluation. A HT-29 xenograft model in nude mice was established to evaluate the in vivo antitumor potency of compound **6d** (hydrochlorate). HT-29 cells (1×10^7) were subcutaneously implanted in the right flanks of male nude mice (BALB/c-nu). When tumor size reached about 100 mm^3, mice were randomized to six per group and were orally administrated with **6d** (hydrochlorate), SAHA or pazopanib for 25 consecutive days. Tumor growth inhibition (TGI) and relative increment ratio (T/C) were calculated at the end of treatment to evaluate the antitumor effects in the aspects of tumor weight and tumor volume, respectively. As shown in Table 7, **6d** (hydrochlorate, 50 mg/kg/d) exhibited potent oral antitumor activity, which was comparable to pazopanib at the same dosage (50 mg/kg/d) and SAHA at the higher dosage (100 mg/kg/d). The tumor growth delay induced by **6d** (hydrochlorate) were visualized by the tumor growth curve in Figure 9A and the final tumor

tissue size in Figure 9B. Moreover, in the mice group treated by **6d** (hydrochlorate), no significant body weight loss and no evident toxic signs in liver and spleen were observed.

Table 7. In Vivo Antitumor Efficacy in HT-29 Xenograft Model

Compd	Administration	T/C (%)[a]	TGI (%)[a]
6d	50 mg/kg/d, PO	65	40
Pazopanib	50 mg/kg/d, PO	61	44
SAHA	100 mg/kg/d, PO	66	39

[a]Compared with the control group, all treated groups showed statistically significant ($P < 0.05$) T/C and TGI by Student's two-tailed t test.

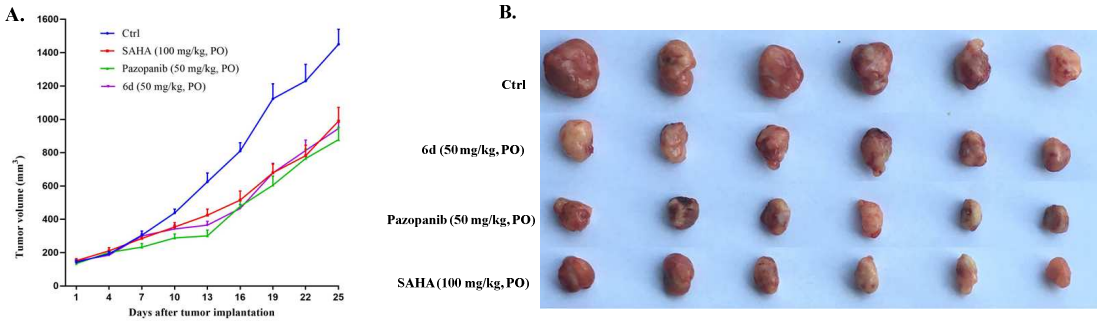

Figure 9. **A.** Growth curve of implanted HT-29 xenograft in nude mice. **B.** Picture of dissected HT-29 tumor tissue.

CONCLUSIONS

In summary, a novel series of pazopanib derivatives simultaneously inhibiting HDAC and VEGFR were rationally designed, synthesized and identified. Among them, one pazopanib-based *ortho*-aminoanilide **6d** and one pazopanib-based hydroxamic acid **13f** exhibited comparable HDACs inhibitory activities to MS-275 and SAHA respectively, which transformed to their potent antiproliferative activities. Compounds **6d** and **13f** also exhibited uncompromised multiple tyrosine kinases inhibitory activities and antiangiogenic potencies compared to pazopanib. Importantly,

compound **6d** possessed desirable pharmacokinetic profiles with the oral bioavailability of 72 % in SD rats and considerable *in vivo* antitumor efficacy in a HT-29 xenograft model. Though **6d** showed no significant advantage over pazopanib in our preliminary in vivo antitumor model, it should be noted that **6d** is of great therapeutic potential for mutant TP53-expressing tumors due to the clinical benefit in a phase I trial of pazopanib plus SAHA. Moreover, based on the encouraging results of another phase I clinical study that combination of pazopanib and HDAC inhibitor resulted in strikingly durable responses in patients with pazopanib-refractory diseases, further evaluation of **6d** in pazopanib-refractory tumor models is warranted. Currently, related in vitro and in vivo studies are in progress in our lab.

EXPERIMENTAL SECTION

Chemistry. The chemical reagents and solvents were purchased from commercial sources and were used without further purification. ^{1}H NMR and ^{13}C NMR spectra were obtained using a Bruker DRX spectrometer at 400 and 100 MHz respectively. Chemical shifts were reported in parts per million (ppm). Multiplicity of ^{1}H NMR signals was reported as singlet (s), doublet (d), triplet (t), quartert (q) and multiplet (m). ESI-MS data was recorded on an API 4000 spectrometer. High resolution mass spectra were conducted by Shandong Analysis and Test Center in Ji'nan. Melting points were determined using open capillary on an uncorrected electrothermal melting points apparatus. HPLC analysis was carried out on an Agilent 1200 with an ODS HYPERSIL column (4.6 mm×250 mm, 5 μm). The flow rate is 1 mL / min. All final compounds achieved a minimum of 95% purity.

***N*-(2-Chloropyrimidin-4-yl)-2,3-dimethyl-2*H*-indazol-6-amine** (**2**). To a stirred solution of **1** (5.00 g, 31.0 mmol) and $NaHCO_3$ (10.4 g, 124 mmol) in EtOH (100 mL) was added 2,4-dichloropyrimidine (13.9 g, 93 mmol) at room temperature. The reaction was stirred at 75 °C for 4 h. The resulting suspension was filtered, and the residue was washed thoroughly with EtOAc. The filtrate was

concentrated under vacuum to leave residue. The residue was triturated with EtOAc to afford compound **2**, pale yellow solid (7.64 g, 90%). Mp: 215-216 ℃. ^{1}H NMR (400 MHz, DMSO-d_6) δ 10.02 (s, 1H, ArNHAr), 8.16 (d, J = 5.9 Hz, 1H, ArH), 7.96 (s, 1H, ArH), 7.63 (d, J = 8.9 Hz, 1H, ArH), 6.98 (dd, J = 8.9, 1.8 Hz, 1H, ArH), 6.78 (d, J = 5.9 Hz, 1H, ArH), 4.01 (s, 3H, NCH_3), 2.58 (s, 3H, $ArCH_3$).

***N*-(2-Chloropyrimidin-4-yl)-*N*,2,3-trimethyl-2*H*-indazol-6-amine** (**3**). To a solution of compound **2** (1.00 g, 3.65 mmol) in DMF (50 mL) was added cesium carbonate (2.38 g, 7.31 mmol). The reaction mixture was stirred for 30 min under nitrogen. Iodomethane (0.78 g, 5.48 mmol) was added and the reaction mixture was stirred at room temperature for 2 h. The reaction mixture was poured into ice cold water and stirred for 30 min. The resulting precipitate was filtered off, washed with water, and air-dried, the crude was recrystallization by EtOAc to afford the desired compound **3**, pale yellow solid (0.84 g, 80%). Mp: 173-174 ℃. ^{1}H NMR (400 MHz, DMSO-d_6) δ 7.95 (d, J = 6.1 Hz, 1H, ArH), 7.80 (dd, J = 0.8, 8.7 Hz, 1H, ArH), 7.51 (dd, J = 0.8, 1.8 Hz, 1H, ArH), 6.88 (dd, J = 1.8, 8.8 Hz, 1H, ArH), 6.24 (d, J = 6.1 Hz, 1H, ArH), 4.06 (s, 3H, NCH_3), 3.42 (s, 3H, NCH_3), 2.63 (s, 3H, $ArCH_3$).

4-((4-((2,3-Dimethyl-2*H*-indazol-6-yl)(methyl)amino)pyrimidin-2-yl)amino)benzoic acid (**4a**). To a solution of **3** (0.50 g, 1.74 mmol) and 4-aminobenzoic acid (0.29 g, 2.09 mmol) in isopropanol (30 mL) was added 2 drops of conc. HCl, and the mixture was heated to reflux with stirring for 4 h. The mixture was cooled to room temperature and the resulting precipitate was collected via filtration and washed with EtOAc, affording compound **4a**, white solid (0.53 g, 79%). Mp: >250 ℃. ^{1}H NMR (400 MHz, DMSO-d_6) δ 12.16 (s, 1H, ArCOOH), 9.80 (s, 1H, ArNHAr), 7.91 (d, J = 6.3 Hz, 1H , ArH), 7.79 (d, J = 8.7 Hz, 3H, ArH), 7.74 (d, J = 8.6 Hz, 2H , ArH), 7.49 (d, J = 1.7 Hz, 1H , ArH), 6.91 (dd, J = 1.8, 8.8 Hz, 1H , ArH), 5.94 (d, J = 6.2 Hz, 1H, ArH), 4.08 (s, 3H, NCH_3), 3.51 (s, 3H, NCH_3), 2.64 (s, 3H, $ArCH_3$). ESI-MS m/z: 387.5 $[M-H]^-$.

Compounds **4b** and **4c** were prepared from compound **3** in a similar manner as described for compound **4a**.

3-((4-((2,3-Dimethyl-2*H*-indazol-6-yl)(methyl)amino)pyrimidin-2-yl)amino)benzoic acid (**4b**). White solid, 81% yield. Mp: >250 ℃. ^{1}H NMR (400 MHz, DMSO-d_6) δ 12.22 (s, 1H, ArCOOH), 9.68 (s, 1H, ArNHAr), 8.52 (s, 1H, ArH), 7.88 (dd, J = 2.1, 7.6 Hz, 1H, ArH), 7.84 (d, J = 6.3 Hz, 1H, ArH), 7.79 (d, J = 8.8 Hz, 1H, ArH), 7.54 (d, J = 7.7 Hz, 1H, ArH), 7.50 (d, J = 1.7 Hz, 1H, ArH), 7.34 (t, J = 7.9 Hz, 1H, ArH), 6.91 (dd, J = 1.8, 8.7 Hz, 1H, ArH), 5.83 (d, J = 6.3 Hz, 1H, ArH), 4.07 (s, 3H, NCH_3), 3.52 (s, 3H, NCH_3), 2.64 (s, 3H, $ArCH_3$). ESI-MS m/z: 387.6 $[M-H]^-$.

5-((4-((2,3-Dimethyl-2*H*-indazol-6-yl)(methyl)amino)pyrimidin-2-yl)amino)-2-methylbenzoic acid (**4c**). White solid, 90% yield. Mp: 230-232 ℃. ESI-MS m/z: 401.6 $[M-H]^-$.

Methyl 4-((4-((2,3-dimethyl-2*H*-indazol-6-yl)(methyl)amino)pyrimidin-2-yl)amino) benzoate (**5a**). To a solution of compound **4a** (0.50 g, 1.29 mmol) in MeOH (50 mL) was added $SOCl_2$ (0.61 g, 5.16 mmol) dropwise at 0 ℃. The mixture was heated to reflux for 4 h. The solvent was evaporated under vacuum. The crude product was recrystallized from isopropanol to obtain **5a**, white solid (0.49 g, 95%). Mp: 198-200 ℃. ^{1}H NMR (400 MHz, DMSO-d_6) δ 9.63 (s, 1H, ArNHAr), 7.92 (d, J = 6.0 Hz, 1H, ArH), 7.83 (d, J = 8.6 Hz, 2H, ArH), 7.78 (d, J = 8.6 Hz, 1H, ArH), 7.72 (d, J = 8.6 Hz, 2H, ArH), 7.46 (dd, J = 0.8, 1.7 Hz, 1H, ArH), 6.89 (dd, J = 1.8, 8.8 Hz, 1H, ArH), 5.91 (d, J = 6.0 Hz, 1H, ArH), 4.07 (s, 3H, NCH_3), 3.80 (s, 3H, $COOCH_3$), 3.49 (s, 3H, NCH_3), 2.64 (s, 3H, $ArCH_3$). ESI-MS m/z: 403.5 $[M+H]^+$.

Compounds **5b** and **5c** were prepared from compounds **4b** and **4c** in a similar manner as described for **5a**, respectively.

Methyl 3-((4-((2,3-dimethyl-2*H*-indazol-6-yl)(methyl)amino)pyrimidin-2-yl)amino)benzoate

(**5b**). White solid. 93% yield. Mp: 192-194 ℃. ^{1}H NMR (400 MHz, DMSO-d_6) δ 9.77-9.61 (m, 1H, ArNHAr), 8.67 (s, 1H, ArH), 7.86 (t, J = 6.4 Hz, 2H, ArH), 7.79 (d, J = 8.7 Hz, 1H, ArH), 7.54 (d, J = 7.7 Hz, 1H, ArH), 7.50 (d, J = 1.7 Hz, 1H, ArH), 7.36 (t, J = 7.9 Hz, 1H, ArH), 6.91 (dd, J = 1.8, 8.7 Hz, 1H, ArH), 5.82 (d, J = 6.3 Hz, 1H, ArH), 4.07 (s, 3H, NCH_3), 3.84 (s, 3H, $COOCH_3$), 3.54 (s, 3H, NCH_3), 2.64 (s, 3H, $ArCH_3$). ESI-MS m/z: 403.5 $[M+H]^+$.

Methyl 5-((4-((2,3-dimethyl-2*H*-indazol-6-yl)(methyl)amino)pyrimidin-2-yl)amino)-2-methylbenzoate (**5c**). White solid. 94% yield. Mp: 218-220 ℃. ESI-MS m/z: 417.6 $[M+H]^+$.

4-((4-((2,3-Dimethyl-2*H*-indazol-6-yl)(methyl)amino)pyrimidin-2-yl)amino)-*N*-hydroxybenzamide (**6a**). KOH (28.55 g, 509 mmol) and $NH_2OH.HCl$ (23.84 g, 343 mmol) were dissolved, respectively, in 70 mL and 120 mL MeOH to get solution A and solution B. Then solution A was added dropwise to solution B. After filtering the precipitate (KCl), a NH_2OK solution was obtained. Compound **5a** (0.20 g, 0.50 mmol) was dissolved in 30 mL NH_2OK solution and stirred for 2 h. After the reaction was complete, it was evaporated under vacuum. The residue was acidified by addition of 1 M HCl to a pH 5-6. The resulting precipitate was collected by filtration and dried to afford compound **6a**, white solid (0.081 g, 40% yield). Mp: 210-212 ℃. ^{1}H NMR (400 MHz, DMSO-d_6) δ 10.99 (s, 1H, OH), 9.49 (s, 1H, ArNHAr), 8.85 (s, 1H, NH), 7.89 (d, J = 6.1 Hz, 1H, ArH), 7.84-7.70 (m, 3H, ArH), 7.59 (d, J = 8.3 Hz, 2H, ArH), 7.46 (s, 1H, ArH), 6.90 (d, J = 8.7 Hz, 1H, ArH), 5.86 (d, J = 6.2 Hz, 1H, ArH), 4.07 (s, 3H, NCH_3), 3.49 (s, 3H, NCH_3), 2.64 (s, 3H, $ArCH_3$). ^{13}C NMR (100 MHz, DMSO-d_6) δ 164.82, 162.88, 159.63, 156.25, 147.45, 144.33, 142.37, 132.64, 127.88, 124.75, 122.21, 120.19, 119.95, 117.88, 114.42, 97.36, 38.42, 37.85, 9.90. HRMS (AP-ESI) m/z calcd for $C_{21}H_{21}N_7O_2$ $[M+H]^+$ 404.1757, found 404.1739. Retention time: 14.1 min, eluted with 40% methanol/60% water (containing 0.1% trifluoroacetic acid).

Compounds **6b** and **6c** were prepared from compounds **5b** and **5c** in a similar manner as described for compound **6a**, respectively.

3-((4-((2,3-Dimethyl-2*H*-indazol-6-yl)(methyl)amino)pyrimidin-2-yl)amino)-*N*-hydroxybenzamide (6b). White solid. 53% yield. Mp: 200-202 ℃. ^{1}H NMR (400 MHz, DMSO-d_6) δ 11.09 (s, 1H, OH), 9.32 (s, 1H, ArNHAr), 8.96 (s, 1H, NH), 8.32 (s, 1H, ArH), 7.91-7.81(m, 2H, ArH), 7.77 (d, J = 8.7 Hz, 1H, ArH), 7.45 (d, J = 1.7 Hz, 1H, ArH), 7.29-7.17 (m, 2H, ArH), 6.89 (dd, J = 1.8, 8.8 Hz, 1H, ArH), 5.77 (d, J = 6.0 Hz, 1H, ArH), 4.06 (s, 3H, NCH_3), 3.50 (s, 3H, NCH_3), 2.63 (s, 3H, $ArCH_3$). ^{13}C NMR (100 MHz, DMSO-d_6) δ 164.95, 162.75, 156.87, 151.57, 147.24, 141.57, 140.33, 133.86, 132.85, 128.91, 122.61, 122.28, 120.43, 120.19, 119.62, 118.87, 114.52, 97.33, 38.98, 37.92, 9.92. HRMS (AP-ESI) m/z calcd for $C_{21}H_{21}N_7O_2$ $[M+H]^+$ 404.1835, found 404.1812. Retention time: 18.8 min, eluted with 36% methanol/64% water (containing 0.1% trifluoroacetic acid).

5-((4-((2,3-Dimethyl-2*H*-indazol-6-yl)(methyl)amino)pyrimidin-2-yl)amino)-*N*-hydroxy-2-methylbenzamide (**6c**). White solid. 57% yield. Mp: 130-132 ℃. ^{1}H NMR (400 MHz, DMSO-d_6) δ 10.76 (s, 1H, OH), 9.21 (s, 1H, ArNHAr), 9.02 (s, 1H, NH), 7.83 (d, J = 6.0 Hz, 1H, ArH), 7.79-7.74 (m, 2H, ArH), 7.71 (dd, J = 2.4, 8.4 Hz, 1H, ArH), 7.44 (d, J = 1.7 Hz, 1H, ArH), 7.04 (d, J = 8.4 Hz, 1H, ArH), 6.88 (dd, J = 1.7, 8.8 Hz, 1H, ArH), 5.75 (d, J = 5.8 Hz, 1H, ArH), 4.06 (s, 3H, NCH_3), 3.47 (s, 3H, NCH_3), 2.63 (s, 3H, $ArCH_3$), 2.23 (s, 3H, $ArCH_3$). ^{13}C NMR (100 MHz, DMSO-d_6) δ 166.03, 162.65, 155.16, 151.56, 146.56, 142.98, 140.13, 135.72, 134.82, 133.61, 132.21, 131.47, 123.39, 122.65, 120.62, 118.89, 114.71, 97.69, 39.45, 37.97, 19.11, 9.94. HRMS (AP-ESI) m/z calcd for $C_{22}H_{23}N_7O_2$ $[M+H]^+$ 418.1991, found 418.1990. Retention time: 14.2 min, eluted with 36% methanol/64% water (containing 0.1% trifluoroacetic acid).

***N*-(2-Aminophenyl)-4-((4-((2,3-dimethyl-2*H*-indazol-6-yl)(methyl)amino)pyrimidin-2-yl)amino)**

benzamide (**6d**). To a solution of **4a** (0.50g, 1.29 mmol) in anhydrous DMF (50 mL) in ice bath, was added 2-(1H-Benzotriazole-1-yl)-1,1,3,3-tetramethyluronium tetrafluoroborate (TBTU, 0.50 g, 1.54 mmol), followed by Et_3N (0.16 g, 1.54 mmol). 30 min later, *o*-diaminobenzene (0.17 g, 1.54 mmol) was added, 12 h later, the solution was diluted by water and extracted with ethyl acetate. The combined organic extract was washed with saturated $NaHCO_3$ and brine, dried over Na_2SO_4 overnight, and the solvent was evaporated under vacuum. The crude product was purified by silica gel column chromatography ($MeOH/CH_2Cl_2$, 1/50-1/20) to afford compound **6d** (0.40 g, 65% yield), white solid. Mp: 138-140 ℃. ^{1}H NMR (400 MHz, DMSO-d_6) δ 9.54 (s, 1H, NH), 9.49 (s, 1H, NH), 7.91 (d, J = 6.0 Hz, 1H, ArH), 7.87 (d, J = 9.0 Hz, 2H, ArH), 7.83 (d, J = 8.8 Hz, 2H, ArH), 7.80-7.76 (m, 1H, ArH), 7.47 (d, J = 2.3 Hz, 1H, ArH), 7.17 (dd, J = 1.5, 7.9 Hz, 1H, ArH), 6.96 (td, J = 1.6, 7.6 Hz, 1H, ArH), 6.91 (dd, J = 1.8, 8.8 Hz, 1H, ArH), 6.79 (dd, J = 1.5, 8.0 Hz, 1H, ArH), 6.60 (td, J = 1.5, 7.5 Hz, 1H, ArH), 5.87 (d, J = 6.0 Hz, 1H, ArH), 4.89 (s, 2H, $ArNH_2$), 4.06 (s, 3H, NCH_3), 3.51 (s, 3H, NCH_3), 2.63 (s, 3H, $ArCH_3$). ^{13}C NMR (100 MHz, DMSO-d_6) δ 165.39, 162.91, 159.45, 156.02, 147.46, 144.54, 143.42, 142.33, 132.64, 128.88, 126.97, 126.63, 126.60, 124.33, 122.23, 120.17, 119.99, 117.79, 116.84, 116.69, 114.46, 97.41, 38.48, 37.85, 9.90. HRMS (AP-ESI) m/z calcd for $C_{27}H_{26}N_8O$ $[M+H]^+$ 479.2230, found 479.2257. Retention time: 8.7 min, eluted with 65% methanol/35% water.

***N*-(2-Aminophenyl)-3-((4-((2,3-dimethyl-2*H*-indazol-6-yl)(methyl)amino)pyrimidin-2-yl)amino) benzamide** (**6e**). Compound **6e** was prepared from compound **4b** in a similar manner as described for compound **6d**. Off-white solid. 43% yield. Mp: 230-232 ℃. ^{1}H NMR (400 MHz, DMSO-d_6) δ 9.60 (s, 1H, NH), 9.37 (s, 1H, NH), 8.49 (s, 1H, ArH), 7.91 (dd, J = 2.2, 8.2 Hz, 1H, ArH), 7.86 (d, J = 6.0 Hz, 1H, ArH), 7.76 (d, J = 8.8 Hz, 1H, ArH), 7.51 (d, J = 7.6 Hz, 1H, ArH), 7.45 (d, J = 1.7 Hz, 1H, ArH), 7.32 (t, J = 7.9 Hz, 1H, ArH), 7.23-7.16 (m, 1H, ArH), 6.97 (td, J = 1.6, 7.6 Hz, 1H, ArH), 6.89 (dd, J =

1.8, 8.8 Hz, 1H, ArH), 6.79 (dd, J = 1.4, 8.0 Hz, 1H, ArH), 6.61 (td, J = 1.5, 7.6 Hz, 1H, ArH), 5.78 (d, J = 6.0 Hz, 1H, ArH), 4.91 (s, 2H, $ArNH_2$), 4.06 (s, 3H, NCH_3), 3.50 (s, 3H, NCH_3), 2.62 (s, 3H, $ArCH_3$). ^{13}C NMR (100 MHz, DMSO-d_6) δ 166.31, 162.85, 159.84, 156.08, 147.44, 143.33, 142.32, 141.73, 135.67, 132.63, 128.61, 126.83, 126.75, 124.10, 122.28, 121.76, 120.11, 119.96, 118.74, 116.81, 116.67, 114.38, 97.12, 38.46, 37.85, 9.89. HRMS (AP-ESI) m/z calcd for $C_{27}H_{26}N_8O$ $[M+H]^+$ 479.2230, found 479.2280. Retention time: 8.9 min, eluted with 65% methanol/35% water.

4-((4-((2,3-Dimethyl-2*H*-indazol-6-yl)(methyl)amino)pyrimidin-2-yl)amino)-*N*-methoxy-*N*-methylbenzamide (**7a**). To a solution of **4a** (0.50g, 1.29 mmol) in anhydrous DMF (50 mL) in ice bath, was added 2-(1H-Benzotriazole-1-yl)-1,1,3,3-tetramethyluronium tetrafluoroborate (TBTU, 0.50 g, 1.54 mmol), followed by Et_3N (0.16 g, 1.54 mmol). 30 min later, N,O-dimethylhydroxylamine hydrochloride (0.15 g, 1.54 mmol) and additional Et_3N (0.16 g, 1.54 mmol) were added, 12 h later, the solution was diluted by water and extracted with ethyl acetate. The combined organic extract was washed with saturated $NaHCO_3$ and brine, dried over Na_2SO_4 overnight, and the solvent was evaporated under vacuum. The crude product was purified by silica gel column chromatography ($MeOH/CH_2Cl_2$, 1/50-1/20) to afford compound **7a** (0.40 g, 72% yield), white solid. Mp: 216-218 ℃. ^1H NMR (400 MHz, DMSO-d_6) δ 9.46 (s, 1H, ArNHAr), 7.90 (d, J = 6.0 Hz, 1H, ArH), 7.82-7.74 (m, 3H, ArH), 7.48 (d, J = 8.6 Hz, 2H, ArH), 7.46 (d, J = 1.4 Hz, 1H, ArH), 6.89 (dd, J = 1.8, 8.8 Hz, 1H, ArH), 5.87 (d, J = 6.0 Hz, 1H, ArH), 4.06 (s, 3H, NCH_3), 3.55 (s, 3H, OCH_3), 3.48 (s, 3H, NCH_3), 3.23 (s, 3H, NCH_3), 2.63 (s, 3H, $ArCH_3$).

3-((4-((2,3-Dimethyl-2*H*-indazol-6-yl)(methyl)amino)pyrimidin-2-yl)amino)-*N*-methoxy-*N*-methylbenzamide (**7b**). Compound **7b** was prepared from compound **4b** in a similar manner as described for compound **7a**. White solid. 71% yield. 185-187 ℃. ^1H NMR (400 MHz, DMSO-d_6) δ

9.36 (s, 1H, ArNHAr), 8.09 (t, J = 1.9 Hz, 1H, ArH), 7.86-7.83 (m, 2H, ArH), 7.76 (d, J = 8.8 Hz, 1H, ArH), 7.50-7.42 (m, 1H, ArH), 7.24 (t, J = 7.9 Hz, 1H, ArH), 7.06 (d, J = 7.6 Hz, 1H, ArH), 6.89 (dd, J = 8.8, 1.8 Hz, 1H, ArH), 5.78 (d, J = 6.0 Hz, 1H, ArH), 4.06 (s, 3H, NCH_3), 3.56 (s, 3H, OCH_3), 3.51 (s, 3H, NCH_3), 3.23 (s, 3H, NCH_3), 2.63 (s, 3H, $ArCH_3$).

4-((4-((2,3-Dimethyl-2*H*-indazol-6-yl)(methyl)amino)pyrimidin-2-yl)amino)benzaldehyde (**8a**). Compound **7a** (1.00 g, 2.32 mmol) was dissolved in anhydrous THF (50 mL) and cooled to -40 ℃. Lithium aluminum hydride (0.26 g, 6.95 mmol) was added in batches. The resulting mixture was stirred at -40 ℃ for 4 h. After the reaction was complete, the mixture was quenched by addition of cold water. Most of the THF was removed under reduced pressure and the residue was diluted with water and extracted with EtOAc. The combined organic layer was washed with brine, dried over $MgSO_4$, filtered and condensed. The crude was purified by silica gel column chromatography ($MeOH/CH_2Cl_2$, 1/50-1/30) to afford compound **8a**, white solid (0.60 g,70% yield). Mp: 242-244 ℃. ^{1}H NMR (400 MHz, DMSO-d_6) δ 9.78-9.77 (m, 2H, ArNHAr and CHO), 7.96-7.93(m, 3H, ArH), 7.78 (d, J = 8.7 Hz, 1H, ArH), 7.69 (d, J = 8.4 Hz, 2H, ArH), 7.47 (d, J = 1.6 Hz, 1H, ArH), 6.90 (dd, J = 1.8, 8.8 Hz, 1H, ArH), 5.92 (d, J = 6.0 Hz, 1H, ArH), 4.07 (s, 3H, NCH_3), 3.50 (s, 3H, NCH_3), 2.64 (s, 3H, $ArCH_3$).

3-((4-((2,3-Dimethyl-2*H*-indazol-6-yl)(methyl)amino)pyrimidin-2-yl)amino)benzaldehyde (**8b**). Compound **8b** was prepared from compound **7b** in a similar manner as described for compound **8a**. White solid. 72% yield. Mp: 238-240 ℃. ^{1}H NMR (400 MHz, DMSO-d_6) δ 9.77 (s, 1H, CHO), 9.50 (s, 1H, ArNHAr), 8.47 (s, 1H, ArH), 7.94-7.92 (m, 1H, ArH), 7.89 (d, J = 5.9 Hz, 1H, ArH), 7.76 (dd, J = 0.8, 8.7 Hz, 1H, ArH), 7.46 (dd, J = 0.7, 1.8 Hz, 1H, ArH), 7.43-7.37 (m, 2H, ArH), 6.90 (dd, J = 1.8, 8.8 Hz, 1H, ArH), 5.85 (d, J = 6.0 Hz, 1H, ArH), 4.06 (s, 3H, NCH_3), 3.50 (s, 3H, NCH_3), 2.63 (s, 3H, $ArCH_3$).

Ethyl (E)-3-(4-((4-((2,3-dimethyl-2*H*-indazol-6-yl)(methyl)amino)pyrimidin-2-yl)amino)phenyl) acrylate (9a). To a solution of triethyl phosphonoacetate (0.32 g, 1.41 mmol) in anhydrous THF (50 mL) cooled to -5-0 ℃ was added NaH (0.01 g, 4.02 mmol). The resulting mixture was stirred for 20 min, followed by the addition of **8a** (0.50 g, 1.34 mmol) in anhydrous THF (50 mL). The mixture was stirred at room temperature for 12 h. After the reaction was complete, the mixture was quenched by 10 % NH_4Cl aqueous solution (50 mL) followed by addition of EtOAc (50 mL). The mixture was stirred for 30 min and stand for layering. The organic layer was concentrated to afford a crude product. The crude was purified by silica gel column chromatography ($MeOH/CH_2Cl_2$, 1/50-1/30 to afford compound **9a,** white solid (0.40 g ,68% yield), Mp: 195-197 ℃, ^1H NMR (400 MHz, DMSO-d_6) δ 9.50 (s, 1H, ArNHAr), 7.89 (d, J = 6.0 Hz, 1H, ArH), 7.83 (d, J = 8.7 Hz, 2H, ArH), 7.78 (dd, J = 0.8, 8.7 Hz, 1H, ArH), 7.58-7.51 (m, 3H, ArH and CH=C), 7.46 (dd, J = 0.8, 1.8 Hz, 1H, ArH), 6.90 (dd, J = 1.8, 8.8 Hz, 1H, ArH), 6.42 (d, J = 16.0 Hz, 1H, CH=C), 5.84 (d, J = 6.0 Hz, 1H, ArH), 4.17 (q, J = 7.1 Hz, 2H, OCH_2), 4.07 (s, 3H, NCH_3), 3.49 (s, 3H, NCH_3), 2.64 (s, 3H, $ArCH_3$), 1.25 (t, J = 7.1 Hz, 3H, CH_3).

Ethyl (E)-3-(3-((4-((2,3-dimethyl-2*H*-indazol-6-yl)(methyl)amino)pyrimidin-2-yl)amino)phenyl) acrylate (**9b**). Compound **9b** was prepared from compound **8b** in a similar manner as described for compound **9a**. White solid. 65% yield. Mp: 198-200 ℃. ^1H NMR (400 MHz, DMSO-d_6) δ 9.25 (s, 1H, ArNHAr), 8.09 (s, 1H, ArH), 7.87 (d, J = 6.0 Hz, 1H, ArH), 7.82-7.78 (m, 1H, ArH), 7.76 (d, J = 8.7 Hz, 1H, ArH), 7.55 (d, J = 16.0 Hz, 1H, CH=C), 7.45 (d, J = 1.7 Hz, 1H, ArH), 7.29-7.20 (m, 2H, ArH), 6.90 (dd, J = 8.7, 1.8 Hz, 1H, ArH), 6.48 (d, J = 16.0 Hz, 1H, CH=C), 5.80 (d, J = 6.0 Hz, 1H, ArH), 4.19 (q, J = 7.1 Hz, 2H, OCH_2), 4.06 (s, 3H, NCH_3), 3.49 (s, 3H, NCH_3), 2.62 (s, 3H, $ArCH_3$), 1.26 (t, J = 7.1 Hz, 3H, CH_3).

Compounds **10a** and **10b** were prepared from compounds **9a** and **9b** in a similar manner as described

for compound **6a**, respectively.

(E)-3-(4-((4-((2,3-Dimethyl-2*H*-indazol-6-yl)(methyl)amino)pyrimidin-2-yl)amino)phenyl)-*N*-hydroxyacrylamide (10a). White solid. 60% yield. Mp:194-196 ℃. ^{1}H NMR (400 MHz, DMSO-d_6) δ 10.65 (s, 1H, OH), 9.42 (s, 1H, ArNHAr), 8.96 (s, 1H, NH), 7.88 (d, J = 5.9 Hz, 1H, ArH), 7.81 (d, J = 8.3 Hz, 2H, ArH), 7.77 (d, J = 8.8 Hz, 1H, ArH), 7.46 (s, 1H, ArH), 7.43-7.32 (m, 3H, ArH and CH=C), 6.95-6.83 (m, 1H, ArH), 6.28 (d, J = 15.7 Hz, 1H, CH=C), 5.83 (d, J = 6.1 Hz, 1H, ArH), 4.07 (s, 3H, NCH_3), 3.49 (s, 3H, NCH_3), 2.64 (s, 3H, $ArCH_3$). ^{13}C NMR (100 MHz, DMSO-d_6) δ 163.60, 162.78, 155.88, 154.15, 147.23, 141.45, 141.01, 138.45, 132.84, 129.08, 128.54, 122.59, 120.24, 119.89, 119.57, 117.38, 114.58, 97.46, 39.10, 37.94, 9.91. HRMS (AP-ESI) m/z calcd for $C_{23}H_{23}N_7O_2$ $[M+H]^+$ 430.1991, found 430.1988. Retention time: 11.6 min, eluted with 42% methanol/58% water (containing 0.1% trifluoroacetic acid).

(E)-3-(3-((4-((2,3-Dimethyl-2*H*-indazol-6-yl)(methyl)amino)pyrimidin-2-yl)amino)phenyl)-*N*-hydroxyacrylamide (**10b**). White solid. 64% yield. Mp: 190-192℃. ^{1}H NMR (400 MHz, DMSO-d_6) δ 10.79 (s, 1H, OH), 9.49 (s, 1H, ArNHAr), 9.03 (s, 1H, NH), 7.99 (s, 1H, ArH), 7.85 (d, J = 6.2 Hz, 1H, ArH), 7.79 (d, J = 8.7 Hz, 1H, ArH), 7.70 (d, J = 8.9 Hz, 1H, ArH), 7.48 (d, J = 1.7 Hz, 1H, ArH), 7.39 (d, J = 15.7 Hz, 1H, CH=C), 7.26 (t, J = 7.8 Hz, 1H, ArH), 7.12 (d, J = 7.6 Hz, 1H, ArH), 6.91 (dd, J = 1.8, 8.8 Hz, 1H, ArH), 6.40 (d, J = 15.7 Hz, 1H, CH=C), 5.83 (d, J = 6.2 Hz, 1H, ArH), 4.07 (s, 3H, NCH_3), 3.51 (s, 3H, NCH_3), 2.63 (s, 3H, $ArCH_3$). ^{13}C NMR (100 MHz, DMSO-d_6) δ 163.17, 162.81, 158.67, 154.11, 147.36, 142.04, 141.52, 139.28, 135.44, 132.72, 129.45, 122.37, 121.21, 120.67, 120.04, 119.94, 119.24, 118.00, 114.42, 97.17, 38.59, 37.87, 9.89. HRMS (AP-ESI) m/z calcd for $C_{23}H_{23}N_7O_2$ $[M-H]^-$ 428.1835, found 428.1852. Retention time: 13.8 min, eluted with 42% methanol/58% water (containing 0.1% trifluoroacetic acid).

Methyl (4-((4-((2,3-dimethyl-2*H*-indazol-6-yl)(methyl)amino)pyrimidin-2-yl)amino) benzoyl) glycinate (**11a**). To a solution of **4a** (1.00 g, 2.58 mmol) in anhydrous DMF (50 mL) in ice bath, was added 2-(1H-Benzotriazole-1-yl)-1,1,3,3-tetramethyluronium tetrafluoroborate (TBTU, 1.00 g, 3.08 mmol), followed by Et_3N (0.32 g, 3.08 mmol). 30 min later, methyl glycinate hydrochloride (0.39 g, 3.08 mmol) and additional Et_3N (0.32 g, 3.08 mmol) were added, 12 h later, the solution was diluted by water and extracted with ethyl acetate. The combined organic extract was washed with saturated $NaHCO_3$ and brine, dried over Na_2SO_4 overnight, and the solvent was evaporated under vacuum. The crude product was purified by silica gel column chromatography ($MeOH/CH_2Cl_2$, 1/50-1/20) to afford compound **11a** (0.86 g 73% yield), white solid. Mp: 170-172 ℃. ^{1}H NMR (400 MHz, DMSO-d_6) δ 9.51 (s, 1H, ArNHAr), 8.72 (t, J = 5.9 Hz, 1H, NH), 7.90 (d, J = 6.0 Hz, 1H, ArH), 7.84 (d, J = 8.6 Hz, 2H, ArH), 7.77 (d, J = 8.7 Hz, 1H, ArH), 7.71 (d, J = 8.5 Hz, 2H, ArH), 7.46 (d, J = 1.7 Hz, 1H, ArH), 6.90 (dd, J = 1.8, 8.8 Hz, 1H, ArH), 5.85 (d, J = 6.1 Hz, 1H, ArH), 4.07 (s, 3H, NCH_3), 3.98 (d, J = 5.8 Hz, 2H, NCH_2CO), 3.65 (s, 3H, $COOCH_3$), 3.50 (s, 3H, NCH_3), 2.64 (s, 3H, $ArCH_3$).

Compounds **11b-11i** were prepared from compounds **4a-4c** in a similar manner as described for compound **11a**.

Methyl 3-(4-((4-((2,3-dimethyl-2*H*-indazol-6-yl)(methyl)amino)pyrimidin-2-yl)amino)benzamido) propanoate (**11b**). White solid. 77% yield. Mp: 220-222 ℃. ^{1}H NMR (400 MHz, DMSO-d_6) δ 9.46 (s, 1H, ArNHAr), 8.32 (t, J = 5.6 Hz, 1H, NH), 7.89 (d, J = 6.0 Hz, 1H, ArH), 7.81 (d, J = 8.6 Hz, 2H, ArH), 7.79-7.75 (m, 1H, ArH), 7.67 (d, J = 8.5 Hz, 2H, ArH), 7.46 (d, J = 1.9 Hz, 1H, ArH), 6.90 (dd, J = 1.8, 8.8 Hz, 1H, ArH), 5.84 (d, J = 6.0 Hz, 1H, ArH), 4.07 (s, 3H, NCH_3), 3.61 (s, 3H, $COOCH_3$), 3.49 (s, 3H, NCH_3), 3.48-3.43 (m, 2H, NCH_2), 2.64 (s, 3H, $ArCH_3$), 2.58 (t, J = 7.0 Hz, 2H, CH_2CO).

Methyl 4-(4-((4-((2,3-dimethyl-2*H*-indazol-6-yl)(methyl)amino)pyrimidin-2-yl)amino)benzamido) butanoate (**11c**). White solid. 79% yield. Mp: 218-220 ℃. ^{1}H NMR (400 MHz, DMSO-d_6) δ 9.44 (s, 1H, ArNHAr), 8.25 (t, J = 5.7 Hz, 1H, NH), 7.89 (d, J = 6.0 Hz, 1H, ArH), 7.81 (d, J = 8.5 Hz, 2H, ArH), 7.77 (d, J = 8.8 Hz, 1H, ArH), 7.68 (d, J = 8.8 Hz, 2H, ArH), 7.46 (d, J = 1.7 Hz, 1H, ArH), 6.90 (dd, J = 1.8, 8.8 Hz, 1H, ArH), 5.84 (d, J = 6.0 Hz, 1H, ArH), 4.07 (s, 3H, NCH_3), 3.58 (s, 3H, $COOCH_3$), 3.49 (s, 3H, NCH_3), 3.25 (q, J = 6.6 Hz, 2H, NCH_2), 2.64 (s, 3H, $ArCH_3$), 2.36 (t, J = 7.4 Hz, 2H, CH_2CO), 1.81-1.73 (m, 2H, CH_2).

Methyl 5-(4-((4-((2,3-Dimethyl-2*H*-indazol-6-yl)(methyl)amino)pyrimidin-2-yl)amino)benzamido) pentanoate (**11d**). White solid. 69% yield. Mp: 222-224 ℃. ^{1}H NMR (400 MHz, DMSO-d_6) δ 9.44 (s, 1H, ArNHAr), 8.22 (t, J = 5.7 Hz, 1H, NH), 7.88 (d, J = 6.0 Hz, 1H, ArH), 7.81 (d, J = 8.7 Hz, 2H, ArH), 7.77 (dd, J = 0.7, 8.7 Hz, 1H, ArH), 7.68 (d, J = 8.6 Hz, 2H, ArH), 7.48-7.44 (m, 1H, ArH), 6.90 (dd, J = 1.7, 8.8 Hz, 1H, ArH), 5.84 (d, J = 6.0 Hz, 1H, ArH), 4.07 (s, 3H, NCH_3), 3.58 (s, 3H, $COOCH_3$), 3.49 (s, 3H, NCH_3), 3.23 (q, J = 6.2 Hz, 2H, NCH_2), 2.64 (s, 3H, $ArCH_3$), 2.34 (t, J = 7.0 Hz, 2H, CH_2CO), 1.61-1.47 (m, 4H, CH_2).

Methyl 6-(4-((4-((2,3-dimethyl-2*H*-indazol-6-yl)(methyl)amino)pyrimidin-2-yl)amino)benzamido) hexanoate (**11e**). White solid. 74% yield. Mp: 208-210 ℃. ^{1}H NMR (400 MHz, DMSO-d_6) δ 9.46 (s, 1H, ArNHAr), 8.22 (t, J = 5.7 Hz, 1H, NH), 7.89 (d, J = 6.0 Hz, 1H, ArH), 7.81 (d, J = 8.5 Hz, 2H, ArH), 7.77 (d, J = 8.7 Hz, 1H, ArH), 7.68 (d, J = 8.5 Hz, 2H, ArH), 7.46 (d, J = 1.7 Hz, 1H, ArH), 6.90 (dd, J = 1.8, 8.8 Hz, 1H, ArH), 5.83 (d, J = 6.0 Hz, 1H, ArH), 4.07 (s, 3H, NCH_3), 3.58 (s, 3H, $COOCH_3$), 3.49 (s, 3H, NCH_3), 3.21 (q, J = 6.6 Hz, 2H, NCH_2), 2.64 (s, 3H, $ArCH_3$), 2.31 (t, J = 7.4 Hz, 2H, CH_2CO), 1.59-1.46 (m, 4H, CH_2), 1.34-1.23 (m, 2H, CH_2).

Methyl 7-(4-((4-((2,3-dimethyl-2*H*-indazol-6-yl)(methyl)amino)pyrimidin-2-

yl)amino)benzamido) heptanoate (**11f**). White solid. 70% yield. Mp: 172-174 ℃. ^{1}H NMR (400 MHz, DMSO-d_6) δ 9.43 (s, 1H, ArNHAr), 8.20 (t, J = 5.6 Hz, 1H, NH), 7.88 (d, J = 6.0 Hz, 1H, ArH), 7.80 (d, J = 8.7 Hz, 2H, ArH), 7.77 (d, J = 8.8 Hz, 1H, ArH), 7.68 (d, J = 8.6 Hz, 2H, ArH), 7.46 (d, J = 1.9 Hz, 1H, ArH), 6.90 (dd, J = 1.8, 8.7 Hz, 1H, ArH), 5.83 (d, J = 6.0 Hz, 1H, ArH), 4.07 (s, 3H, NCH_3), 3.58 (s, 3H, $COOCH_3$), 3.49 (s, 3H, NCH_3), 3.21 (q, J = 6.6 Hz, 2H, NCH_2), 2.64 (s, 3H, $ArCH_3$), 2.30 (t, J = 7.4 Hz, 2H, CH_2CO), 1.60-1.45 (m, 4H, CH_2), 1.35-1.23 (m, 4H, CH_2).

Methyl 8-(4-((4-((2,3-dimethyl-2*H*-indazol-6-yl)(methyl)amino)pyrimidin-2-yl)amino)benzamido) octanoate (**11g**). White solid. 75% yield. Mp: 168-170 ℃. ^{1}H NMR (400 MHz, DMSO-d_6) δ 9.43 (s, 1H, ArNHAr), 8.19 (t, J = 5.7 Hz, 1H, NH), 7.88 (d, J = 6.0 Hz, 1H, ArH), 7.81 (d, J = 8.5 Hz, 2H, ArH), 7.77 (d, J = 8.7 Hz, 1H, ArH), 7.68 (d, J = 8.5 Hz, 2H, ArH), 7.46 (d, J = 1.7 Hz, 1H, ArH), 6.90 (dd, J = 1.8, 8.8 Hz, 1H, ArH), 5.84 (d, J = 6.0 Hz, 1H, ArH), 4.07 (s, 3H, NCH_3), 3.58 (s, 3H, $COOCH_3$), 3.49 (s, 3H, NCH_3), 3.22 (q, J = 6.6 Hz, 2H, NCH_2), 2.64 (s, 3H, $ArCH_3$), 2.29 (t, J = 7.4 Hz, 2H, CH_2CO), 1.60-1.40 (m, 4H, CH_2), 1.39-1.20(m, 6H, CH_2).

Methyl 6-(3-((4-((2,3-dimethyl-2*H*-indazol-6-yl)(methyl)amino)pyrimidin-2-yl)amino)benzamido) hexanoate (**11h**). White solid. 80% yield. Mp: 210-212 ℃. ^{1}H NMR (400 MHz, DMSO-d_6) δ 9.32 (s, 1H, ArNHAr), 8.40-8.30 (m, 2H, NH and ArH), 7.84 (d, J = 5.9 Hz, 1H, ArH), 7.81 (dd, J = 2.0, 8.1 Hz, 1H, ArH), 7.77 (d, J = 8.7 Hz, 1H, ArH), 7.45 (d, J = 1.7 Hz, 1H, ArH), 7.31 (dt, J = 1.4, 7.7 Hz, 1H, ArH), 7.25 (t, J = 7.8 Hz, 1H, ArH), 6.89 (dd, J = 1.8, 8.8 Hz, 1H, ArH), 4.06 (s, 3H, NCH_3), 3.56 (s, 3H, $COOCH_3$), 3.50 (s, 3H, NCH_3), 3.22 (q, J = 6.7 Hz, 2H, NCH_2), 2.63 (s, 3H, $ArCH_3$), 2.30 (t, J = 7.4 Hz, 2H, CH_2CO), 1.60-1.45 (m, 4H, CH_2), 1.38-1.18 (m, 2H, CH_2).

Methyl 6-(5-((4-((2,3-dimethyl-2*H*-indazol-6-yl)(methyl)amino)pyrimidin-2-yl)amino)-2-methylben-zamido)hexanoate (**11i**). White solid. 76% yield. Mp: 190-192 ℃. ^{1}H NMR (400 MHz,

DMSO-d_6) δ 9.20 (s, 1H, ArNHAr), 8.17 (t, J = 5.7 Hz, 1H, NH), 7.85 (d, J = 2.3 Hz, 1H, ArH), 7.82 (d, J = 6.0 Hz, 1H, ArH), 7.76 (d, J = 8.7 Hz, 1H, ArH), 7.64 (dd, J = 2.4, 8.3 Hz, 1H, ArH), 7.44 (d, J = 1.7 Hz, 1H, ArH), 7.03 (d, J = 8.4 Hz, 1H, ArH), 6.88 (dd, J = 1.8, 8.8 Hz, 1H, ArH), 5.73 (d, J = 6.0 Hz, 1H, ArH), 4.06 (s, 3H, NCH_3), 3.56 (s, 3H, $COOCH_3$), 3.46 (s, 3H, NCH_3), 3.17 (q, J = 6.6 Hz, 2H, NCH_2), 2.63 (s, 3H, $ArCH_3$), 2.30 (t, J = 7.4 Hz, 2H, CH_2CO), 2.22 (s, 3H, $ArCH_3$), 1.58-1.44 (m, 4H, CH_2), 1.35-1.27 (m, 2H, CH_2).

(4-((4-((2,3-Dimethyl-2*H*-indazol-6-yl)(methyl)amino)pyrimidin-2-yl)amino)benzoyl)glycine (**12a**). To a solution of **11a** (1.00 g, 2.18 mmol) in methanol (30 mL) was added 3 M NaOH (5 mL). The resulting mixture was stirred at room temperature for 4 h. After the reaction was complete, it was evaporated under vacuum. The residue was acidified by addition of 1 M HCl to a pH 5-6. The precipitated solid was collected by filtration and washed with ice water, dried in vacuum to afford compound **12a**, White solid (0.81 g, 84% yield), Mp: >250 ℃. ^{1}H NMR (400 MHz, DMSO-d_6) δ 12.50 (s, 1H, COOH), 9.65 (s, 1H, ArNHAr), 8.61 (t, J = 5.9 Hz, 1H, NH, ArH), 7.89 (d, J = 6.2 Hz, 1H, ArH), 7.81-7.78 (m, 3H, ArH), 7.73 (d, J = 8.5 Hz, 2H, ArH), 7.48 (d, J = 1.6 Hz, 1H, ArH), 6.91 (dd, J = 8.8, 1.8 Hz, 1H, ArH), 5.89 (d, J = 6.2 Hz, 1H, ArH), 4.07 (s, 3H, NCH_3), 3.90 (d, J = 5.8 Hz, 2H, NCH_2CO), 3.51 (s, 3H, NCH_3), 2.64 (s, 3H, $ArCH_3$).

Compounds **12b**-**12g** were prepared from compounds **11b**-**11g** in a similar manner as described for compound **12a**, respectively.

3-(4-((4-((2,3-Dimethyl-2*H*-indazol-6-yl)(methyl)amino)pyrimidin-2-yl)amino)benzamido)propanoic acid (**12b**). White solid. 83% yield. Mp: 218-220 ℃. ^{1}H NMR (400 MHz, DMSO-d_6) δ 12.20 (s, 1H), 9.45 (s, 1H), 8.34 (t, J = 5.6 Hz, 1H), 7.89 (d, J = 6.0 Hz, 1H), 7.81 (d, J = 8.6 Hz, 2H), 7.77 (d, J = 8.3 Hz, 1H), 7.67 (d, J = 8.6 Hz, 2H), 7.46 (d, J = 1.9 Hz, 1H), 6.89

(dd, J = 1.8, 8.8 Hz, 1H), 5.84 (d, J = 6.0 Hz, 1H), 4.07 (s, 3H), 3.49 (s, 3H), 3.47-3.42 (m, 2H), 2.64 (s, 3H), 2.48 (t, J = 7.1 Hz, 2H).

4-(4-((4-((2,3-Dimethyl-2*H*-indazol-6-yl)(methyl)amino)pyrimidin-2-yl)amino)benzamido) butanoic acid (**12c**).White solid. 88% yield. Mp: 169-171 ℃. ^{1}H NMR (400 MHz, DMSO-d_6) δ 12.10 (s, 1H, COOH), 9.45 (s, 1H, ArNHAr), 8.35 (t, J = 5.6 Hz, 1H, NH), 7.89 (d, J = 6.0 Hz, 1H, ArH), 7.81 (d, J = 8.5 Hz, 2H, ArH), 7.77 (d, J = 8.7 Hz, 1H, ArH), 7.71 (d, J = 8.5 Hz, 2H, ArH), 7.46 (d, J = 1.7 Hz, 1H, ArH), 6.90 (dd, J = 8.8, 1.8 Hz, 1H, ArH), 5.84 (d, J = 6.0 Hz, 1H, ArH), 4.07 (s, 3H, NCH_3), 3.49 (s, 3H, NCH_3), 3.25 (q, J = 6.5 Hz, 2H, NCH_2), 2.64 (s, 3H, $ArCH_3$), 2.27 (t, J = 7.4 Hz, 2H, CH_2CO), 1.78-1.71 (m, 2H, CH_2).

5-(4-((4-((2,3-Dimethyl-2*H*-indazol-6-yl)(methyl)amino)pyrimidin-2-yl)amino)benzamido)pentanoic acid (**12d**). White solid. 87% yield. Mp: 184-186 ℃. ^{1}H NMR (400 MHz, DMSO-d_6) δ 12.09 (s, 1H, COOH), 9.43 (s, 1H, ArNHAr), 8.22 (t, J = 5.7 Hz, 1H, NH), 7.89 (d, J = 6.0 Hz, 1H, ArH), 7.80 (d, J = 8.6 Hz, 2H, ArH), 7.77 (d, J = 8.8 Hz, 1H, ArH), 7.68 (d, J = 8.5 Hz, 2H, ArH), 7.46 (d, J = 1.7 Hz, 1H, ArH), 6.90 (dd, J = 8.8, 1.8 Hz, 1H, ArH), 5.84 (d, J = 6.0 Hz, 1H, ArH), 4.07 (s, 3H, NCH_3), 3.49 (s, 3H, NCH_3), 3.24-3.21 (m, 2H, NCH_2), 2.64 (s, 3H, $ArCH_3$), 2.24 (t, J = 7.4 Hz, 2H, CH_2CO), 1.56-1.51 (m, 4H, CH_2).

6-(4-((4-((2,3-Dimethyl-2*H*-indazol-6-yl)(methyl)amino)pyrimidin-2-yl)amino)benzamido)hexanoic acid (**12e**). White solid. 81% yield. Mp: 190-192 ℃. ^{1}H NMR (400 MHz, DMSO-d_6) δ 12.04 (s, 1H, COOH), 9.44 (s, 1H, ArNHAr), 8.26 (t, J = 5.7 Hz, 1H, NH), 7.89 (d, J = 6.0 Hz, 1H, ArH), 7.81 (d, J = 8.5 Hz, 2H, ArH), 7.77 (d, J = 8.7 Hz, 1H, ArH), 7.70 (d, J = 8.5 Hz, 2H, ArH), 7.46 (d, J = 1.7 Hz, 1H, ArH), 6.90 (dd, J = 8.8, 1.8 Hz, 1H, ArH), 5.84 (d, J = 6.0 Hz, 1H, ArH), 4.07 (s, 3H, NCH_3), 3.49 (s, 3H, NCH_3), 3.22 (q, J = 6.7 Hz, 2H, NCH_2), 2.64 (s, 3H, $ArCH_3$),

2.19 (t, J = 7.3 Hz, 2H, CH_2CO), 1.56-1.47 (m, 4H, CH_2), 1.34-1.23 (m, 2H, CH_2).

7-(4-((4-((2,3-Dimethyl-2*H*-indazol-6-yl)(methyl)amino)pyrimidin-2-yl)amino)benzamido)heptanoic acid (**12f**). White solid. 89% yield. Mp: 197-199 ℃. ^{1}H NMR (400 MHz, DMSO-d_6) δ 11.97 (s, 1H, COOH), 9.43 (s, 1H, ArNHAr), 8.19 (t, J = 5.6 Hz, 1H, NH), 7.88 (d, J = 6.0 Hz, 1H, ArH), 7.80 (d, J = 8.7 Hz, 2H, ArH), 7.77 (d, J = 8.8 Hz, 1H, ArH), 7.68 (d, J = 8.6 Hz, 2H, ArH), 7.46 (d, J = 1.6 Hz, 1H, ArH), 6.90 (dd, J = 8.8, 1.8 Hz, 1H, ArH), 5.84 (d, J = 6.0 Hz, 1H, ArH), 4.07 (s, 3H, NCH_3), 3.49 (s, 3H, NCH_3), 3.21 (q, J = 6.7 Hz, 2H, NCH_2), 2.64 (s, 3H, $ArCH_3$), 2.20 (t, J = 7.3 Hz, 2H, CH_2CO), 1.57-1.43 (m, 4H, CH_2), 1.35-1.25 (m, 4H, CH_2).

8-(4-((4-((2,3-Dimethyl-2*H*-indazol-6-yl)(methyl)amino)pyrimidin-2-yl)amino)benzamido)octanoic acid (**12g**). White solid. 90% yield. Mp: 257-259 ℃. ^{1}H NMR (400 MHz, DMSO-d_6) δ 11.91 (s, 1H, COOH), 9.52 (s, 1H, ArNHAr), 8.20 (t, J = 5.7 Hz, 1H, NH), 7.88 (d, J = 6.1 Hz, 1H, ArH), 7.80-7.77 (m, 3H, ArH), 7.69 (d, J = 8.5 Hz, 2H, ArH), 7.47 (d, J = 1.7 Hz, 1H, ArH), 6.90 (dd, J = 8.8, 1.8 Hz, 1H, ArH), 5.86 (d, J = 6.1 Hz, 1H, ArH), 4.07 (s, 3H, NCH_3), 3.50 (s, 3H, NCH_3), 3.22 (q, J = 6.7 Hz, 2H, NCH_2), 2.64 (s, 3H, $ArCH_3$), 2.19 (t, J = 7.3 Hz, 2H, CH_2CO), 1.53-1.46 (m, 4H, CH_2), 1.31-1.23 (m, 6H, CH_2).

Compounds **13a-13i** were prepared from compounds **11a-11i** in a similar manner as described for compound **6a**, respectively.

4-((4-((2,3-Dimethyl-2*H*-indazol-6-yl)(methyl)amino)pyrimidin-2-yl)amino)-*N*-(2-(hydroxyamino)-2-oxoethyl)benzamide (**13a**). White solid. 61% yield. Mp: 216-218 ℃. ^{1}H NMR (400 MHz, DMSO-d_6) δ 10.53 (s, 1H, OH), 9.46 (s, 1H, ArNHAr), 8.77 (s, 1H, NH), 8.45 (s, 1H, NH), 7.89 (d, J = 5.9 Hz, 1H, ArH), 7.82 (d, J = 8.5 Hz, 2H, ArH), 7.77 (d, J = 8.7 Hz, 1H, ArH), 7.72 (d, J = 8.4 Hz, 2H, ArH), 7.46 (d, J = 1.8 Hz, 1H, ArH), 6.90 (dd, J = 1.8, 8.8 Hz, 1H, ArH), 5.85 (d, J = 6.0

Hz, 1H, ArH), 4.07 (s, 3H, NCH_3), 3.76 (d, J = 5.8 Hz, 2H, NCH_2CO), 3.49 (s, 3H, NCH_3), 2.64 (s, 3H, $ArCH_3$). ^{13}C NMR (100 MHz, DMSO-d_6) δ 166.65, 162.88, 159.65, 156.28, 147.45, 144.48, 142.36, 132.64, 128.42, 126.13, 122.21, 120.18, 119.96, 117.70, 114.43, 97.38, 41.00, 38.42, 37.85, 9.90. HRMS (AP-ESI) m/z calcd for $C_{23}H_{24}N_8O_3$ $[M-H]^-$ 459.1971, found 459.1921. Retention time: 15.3 min, eluted with 35% methanol/65% water (containing 0.1% trifluoroacetic acid).

4-((4-((2,3-Dimethyl-2*H*-indazol-6-yl)(methyl)amino)pyrimidin-2-yl)amino)-*N*-(3-(hydroxyamino)-3-oxopropyl)benzamide (**13b**). White solid. 60% yield. Mp: 218-220℃. ^1H NMR (400 MHz, DMSO-d_6) δ 10.44 (s, 1H, OH), 9.44 (s, 1H, ArNHAr), 8.73 (s, 1H, NH), 8.28 (t, J = 5.7 Hz, 1H, NH), 7.88 (d, J = 6.0 Hz, 1H, ArH), 7.81 (d, J = 8.6 Hz, 2H, ArH), 7.77 (d, J = 8.3 Hz, 1H, ArH), 7.67 (d, J = 8.6 Hz, 2H, ArH), 7.46 (dd, J = 0.8, 1.8 Hz, 1H, ArH), 6.89 (dd, J = 1.8, 8.8 Hz, 1H, ArH), 5.84 (d, J = 6.0 Hz, 1H, ArH), 4.07 (s, 3H, NCH_3), 3.49 (s, 3H, NCH_3), 3.43 (q, J = 6.7 Hz, 2H, NCH_2), 2.64 (s, 3H, $ArCH_3$), 2.25 (t, J = 7.3 Hz, 2H, CH_2CO). ^{13}C NMR (100 MHz, DMSO-d_6) δ 167.84, 166.38, 162.87, 159.65, 156.28, 147.45, 144.33, 142.35, 132.64, 128.16, 126.52, 122.21, 120.17, 119.96, 117.73, 114.42, 97.35, 38.42, 37.85, 36.43, 33.07, 9.90. HRMS (AP-ESI) m/z calcd for $C_{24}H_{26}N_8O_3$ $[M-H]^-$ 473.2050, found 473.2065. Retention time: 13.7 min, eluted with 38% methanol/62% water (containing 0.1% trifluoroacetic acid).

4-((4-((2,3-Dimethyl-2*H*-indazol-6-yl)(methyl)amino)pyrimidin-2-yl)amino)-*N*-(4-(hydroxyamino)-4-oxobutyl)benzamide (**13c**). White solid. 51% yield. Mp: 199-201 ℃. ^1H NMR (400 MHz, DMSO-d_6) δ 10.39 (d, J = 1.8 Hz, 1H, OH), 9.44 (s, 1H, ArNHAr), 8.70 (d, J = 1.8 Hz, 1H, NH), 8.25 (t, J = 5.7 Hz, 1H, NH), 7.89 (d, J = 6.0 Hz, 1H, ArH), 7.81 (d, J = 8.6 Hz, 2H, ArH), 7.77 (d, J = 8.5 Hz, 1H, ArH), 7.69 (d, J = 8.5 Hz, 2H, ArH), 7.46 (d, J = 2.0 Hz, 1H, ArH), 6.90 (dd, J = 1.8, 8.8 Hz, 1H, ArH), 5.84 (d, J = 6.0 Hz, 1H, ArH), 4.07 (s, 3H, NCH_3), 3.49 (s, 3H, NCH_3), 3.22 (q,

J = 6.6 Hz, 2H, NCH_2), 2.64 (s, 3H, $ArCH_3$), 2.01 (t, J = 7.5 Hz, 2H, CH_2CO), 1.77-1.69 (m, 2H, CH_2). ^{13}C NMR (100 MHz, DMSO-d_6) δ 169.39, 166.39, 162.88, 159.64, 156.26, 147.45, 144.24, 142.36, 132.63, 128.17, 126.72, 122.21, 120.18, 119.96, 117.74, 114.42, 97.32, 39.27, 38.42, 37.85, 30.53, 25.92, 9.90. HRMS (AP-ESI) m/z calcd for $C_{25}H_{28}N_8O_3$ $[M-H]^-$ 487.2206, found 487.2209. Retention time: 15.8 min, eluted with 38% methanol/62% water (containing 0.1% trifluoroacetic acid).

4-((4-((2,3-Dimethyl-2*H*-indazol-6-yl)(methyl)amino)pyrimidin-2-yl)amino)-*N*-(5-(hydroxyamino)-5-oxopentyl)benzamide (**13d**). White solid. 55% yield. Mp: 227-229 ℃. ^1H NMR (400 MHz, DMSO-d_6) δ 10.35 (d, J = 1.6 Hz, 1H, OH), 9.43 (s, 1H, ArNHAr), 8.66 (d, J = 1.8 Hz, 1H, NH), 8.22 (t, J = 5.7 Hz, 1H, NH), 7.88 (d, J = 5.9 Hz, 1H, ArH), 7.81 (d, J = 8.7 Hz, 2H, ArH), 7.77 (d, J = 8.8 Hz, 1H, ArH), 7.68 (d, J = 8.5 Hz, 2H, ArH), 7.46 (d, J = 1.7 Hz, 1H, ArH), 6.90 (dd, J = 1.8, 8.8 Hz, 1H, ArH), 5.84 (d, J = 6.0 Hz, 1H, ArH), 4.07 (s, 3H, NCH_3), 3.49 (s, 3H, NCH_3), 3.22 (q, J = 6.2 Hz, 2H, NCH_2), 2.64 (s, 3H, $ArCH_3$), 1.98 (t, J = 6.8 Hz, 2H, CH_2CO), 1.57-1.48 (m, 4H, CH_2). ^{13}C NMR (100 MHz, DMSO-d_6) δ 169.50, 166.28, 162.87, 159.66, 156.28, 147.45, 144.20, 142.36, 132.63, 128.15, 126.80, 122.21, 120.18, 119.95, 117.73, 114.41, 97.31, 39.25, 38.42, 37.85, 32.53, 29.40, 23.24, 9.90. HRMS (AP-ESI) m/z calcd for $C_{26}H_{30}N_8O_3$ $[M-H]^-$ 501.2363, found 501.2381. Retention time: 13.4 min, eluted with 40% methanol/60% water (containing 0.1% trifluoroacetic acid).

4-((4-((2,3-Dimethyl-2*H*-indazol-6-yl)(methyl)amino)pyrimidin-2-yl)amino)-*N*-(6-(hydroxyamino)-6-oxohexyl)benzamide (**13e**). White solid. 53% yield. Mp: 164-166 ℃. ^1H NMR (400 MHz, DMSO-d_6) δ 10.35 (s, 1H, OH), 9.46 (s, 1H, ArNHAr), 8.67 (d, J = 1.8 Hz, 1H, NH), 8.22 (t, J = 5.7 Hz, 1H, NH), 7.88 (d, J = 6.0 Hz, 1H, ArH), 7.81 (d, J = 8.6 Hz, 2H, ArH), 7.78 (d, J = 8.8 Hz, 1H, ArH), 7.68 (d, J = 8.6 Hz, 2H, ArH), 7.46 (d, J = 1.8 Hz, 1H, ArH), 6.90 (dd, J = 1.8, 8.8 Hz, 1H, ArH), 5.84 (d, J = 6.0 Hz, 1H, ArH), 4.07 (s, 3H, NCH_3), 3.49 (s, 3H, NCH_3), 3.21 (q, J = 6.7 Hz,

2H, NCH_2), 2.64 (s, 3H, $ArCH_3$), 1.95 (t, J = 7.4 Hz, 2H, CH_2CO), 1.56-1.49 (m, 4H, CH_2), 1.39-1.28 (m, 2H, CH_2). ^{13}C NMR (100 MHz, DMSO-d_6) δ 169.54, 166.24, 162.86, 159.33, 155.77, 147.43, 144.02, 142.28, 132.65, 128.16, 126.97, 122.24, 120.13, 119.98, 117.84, 114.42, 97.33, 39.45, 38.48, 37.86, 32.72, 29.51, 26.62, 25.42, 9.90. HRMS (AP-ESI) m/z calcd for $C_{27}H_{32}N_8O_3$ $[M-H]^-$ 515.2519, found 515.2543. Retention time: 13.3 min, eluted with 45% methanol/55% water (containing 0.1% trifluoroacetic acid).

4-((4-((2,3-Dimethyl-2*H*-indazol-6-yl)(methyl)amino)pyrimidin-2-yl)amino)-*N*-(7-(hydroxyamino)-7-oxoheptyl)benzamide (**13f**). White solid. 57% yield. Mp: 157-159 ℃. ^1H NMR (400 MHz, DMSO-d_6) δ 10.33 (s, 1H, OH), 9.43 (s, 1H, ArNHAr), 8.65 (s, 1H, NH), 8.19 (t, J = 5.6 Hz, 1H, NH), 7.88 (d, J = 6.0 Hz, 1H, ArH), 7.80 (d, J = 8.6 Hz, 2H, ArH), 7.77 (dd, J = 0.8, 8.7 Hz, 1H, ArH), 7.68 (d, J = 8.5 Hz, 2H, ArH), 7.46 (dd, J = 0.8, 1.8 Hz, 1H, ArH), 6.90 (dd, J = 1.7, 8.8 Hz, 1H, ArH), 5.84 (d, J = 5.9 Hz, 1H, ArH), 4.07 (s, 3H, NCH_3), 3.49 (s, 3H, NCH_3), 3.21 (q, J = 6.7 Hz, 2H, NCH_2), 2.64 (s, 3H, $ArCH_3$), 1.94 (t, J = 7.3 Hz, 2H, CH_2CO), 1.55-1.43 (m, 4H, CH_2), 1.33-1.23 (m, 4H, CH_2). ^{13}C NMR (100 MHz, DMSO-d_6) δ 169.55, 166.27, 162.87, 159.67, 156.28, 147.45, 144.18, 142.36, 132.63, 128.13, 126.85, 122.20, 120.19, 119.95, 117.73, 114.41, 97.30, 39.51, 38.42, 37.85, 32.72, 29.66, 28.85, 26.73, 25.58, 9.90. HRMS (AP-ESI) m/z calcd for $C_{28}H_{34}N_8O_3$ $[M-H]^-$ 529.2676, found 529.2696. Retention time: 15.2 min, eluted with 45% methanol/55% water (containing 0.1% trifluoroacetic acid).

4-((4-((2,3-Dimethyl-2*H*-indazol-6-yl)(methyl)amino)pyrimidin-2-yl)amino)-*N*-(8-(hydroxyamino)-8-oxooctyl)benzamide (13g). White solid. 53% yield. Mp: 200-202 ℃. ^1H NMR (400 MHz, DMSO-d_6) δ 10.34 (s, 1H, OH), 9.45 (s, 1H, ArNHAr), 8.67 (s, 1H, NH), 8.21 (t, J = 5.6 Hz, 1H, NH), 7.88 (d, J = 6.0 Hz, 1H, ArH), 7.81 (d, J = 8.6 Hz, 2H, ArH), 7.77 (d, J = 8.5 Hz, 1H,

ArH), 7.68 (d, *J* = 8.5 Hz, 2H, ArH), 7.46 (d, *J* = 1.5 Hz, 1H, ArH), 6.90 (dd, *J* = 1.8, 8.8 Hz, 1H, ArH), 5.83 (d, *J* = 6.0 Hz, 1H, ArH), 4.07 (s, 3H, NCH_3), 3.49 (s, 3H, NCH_3), 3.21 (q, *J* = 6.6 Hz, 2H, NCH_2), 2.64 (s, 3H, $ArCH_3$), 1.93 (t, *J* = 7.4 Hz, 2H, CH_2CO), 1.55-1.40 (m, 4H, CH_2), 1.32-1.15 (m, 6H, CH_2). ^{13}C NMR (100 MHz, DMSO-d_6) δ 169.55, 166.26, 162.87, 159.67, 156.28, 147.45, 144.18, 142.36, 132.62, 128.13, 126.85, 122.20, 120.19, 119.95, 117.74, 114.41, 97.30, 39.45, 38.42, 37.84, 32.72, 29.74, 29.04, 28.99, 26.91, 25.57, 9.90. HRMS (AP-ESI) m/z calcd for $C_{29}H_{36}N_8O_3$ $[M-H]^-$ 543.2832, found 543.2860. Retention time: 18.3 min, eluted with 47% methanol/53% water (containing 0.1% trifluoroacetic acid).

3-((4-((2,3-Dimethyl-2*H*-indazol-6-yl)(methyl)amino)pyrimidin-2-yl)amino)-*N*-(6-(hydroxyamino)-6-oxohexyl)benzamide (13h). White solid. 54% yield. Mp: 147-149 ℃. ^1H NMR (400 MHz, DMSO-d_6) δ 10.34 (s, 1H, OH), 9.31 (s, 1H, ArNHAr), 8.67 (d, *J* = 1.8 Hz, 1H, NH), 8.39-8.27 (m, 2H, NH and ArH), 7.84 (d, *J* = 6.0 Hz, 1H, ArH), 7.81 (d, *J* = 2.0 Hz, 1H, ArH), 7.77 (d, *J* = 8.8 Hz, 1H, ArH), 7.45 (d, *J* = 1.7 Hz, 1H, ArH), 7.31 (dt, *J* = 1.5, 7.8 Hz, 1H, ArH), 7.25 (t, *J* = 7.8 Hz, 1H, ArH), 6.89 (dd, *J* = 1.8, 8.8 Hz, 1H, ArH), 5.76 (d, *J* = 6.0 Hz, 1H, ArH), 4.07 (s, 3H, NCH_3), 3.50 (s, 3H, NCH_3), 3.22 (q, *J* = 6.7 Hz, 2H, NCH_2), 2.63 (s, 3H, $ArCH_3$), 1.94 (t, *J* = 7.4 Hz, 2H, CH_2CO), 1.55-1.47 (m, 4H, CH_2), 1.30-1.23 (m, 2H, CH_2). ^{13}C NMR (100 MHz, DMSO-d_6) δ 169.52, 167.09, 162.83, 159.80, 156.00, 147.44, 142.33, 141.60, 135.83, 132.64, 128.49, 122.27, 121.45, 120.10, 119.95, 119.53, 118.40, 114.37, 97.07, 39.47, 38.42, 37.84, 32.72, 29.41, 26.59, 25.41, 9.89. HRMS (AP-ESI) m/z calcd for $C_{27}H_{32}N_8O_3$ $[M-H]^-$ 515.2519, found 515.2545. Retention time: 12.3 min, eluted with 45% methanol/55% water (containing 0.1% trifluoroacetic acid).

5-((4-((2,3-Dimethyl-2*H*-indazol-6-yl)(methyl)amino)pyrimidin-2-yl)amino)-*N*-(6-(hydroxyamino)-6-oxohexyl)-2-methylbenzamide (13i). White solid. 56% yield. Mp: 150-152 ℃. ^1H

NMR (400 MHz, DMSO-d_6) δ 10.35 (s, 1H, OH), 9.19 (s, 1H, ArNHAr), 8.68 (s, 1H, NH), 8.17 (t, J = 5.7 Hz, 1H, NH), 7.84-7.82 (m, 2H, ArH), 7.76 (d, J = 8.7 Hz, 1H, ArH), 7.65 (dd, J = 2.4, 8.3 Hz, 1H, ArH), 7.44 (d, J = 1.8 Hz, 1H, ArH), 7.03 (d, J = 8.4 Hz, 1H, ArH), 6.88 (dd, J = 1.8, 8.8 Hz, 1H, ArH), 5.74 (d, J = 6.0 Hz, 1H, ArH), 4.06 (s, 3H, NCH_3), 3.47 (s, 3H, NCH_3), 3.17 (q, J = 6.6 Hz, 2H, NCH_2), 2.63 (s, 3H, $ArCH_3$), 2.22 (s, 3H, $ArCH_3$), 1.94 (t, J = 7.4 Hz, 2H, CH_2CO), 1.54-1.44 (m, 4H, CH_2), 1.32-1.26 (m, 2H, CH_2).

^{13}C NMR (100 MHz, DMSO-d_6) δ 169.77, 169.48, 162.83, 159.97, 156.20, 147.44, 142.38, 139.16, 138.15, 132.63, 130.56, 126.86, 122.23, 120.14, 119.93, 119.52, 117.52, 114.35, 96.79, 39.12, 38.32, 37.84, 32.71, 29.41, 26.56, 25.37, 19.01, 9.89. HRMS (AP-ESI) m/z calcd for $C_{28}H_{34}N_8O_3$ $[M-H]^-$ 529.2676, found 529.2693. Retention time: 15.1 min, eluted with 44% methanol/56% water (containing 0.1% trifluoroacetic acid).

Compounds **14a-14g** were prepared from compounds **12a-12g** in a similar manner as described for compound **6d**, respectively.

***N*-(2-((2-Aminophenyl)amino)-2-oxoethyl)-4-((4-((2,3-dimethyl-2*H*-indazol-6-yl)(methyl)amino) pyrimidin-2-yl)amino)benzamide (14a)**. Pale yellow solid. 39% yield. Mp: 178-180 ℃. ^{1}H NMR (600 MHz, DMSO-d_6) δ 9.41 (s, 1H, ArNHAr), 9.16 (s, 1H, ArNHCO), 8.54 (s, 1H, NH), 7.90 (d, J = 6.1 Hz, 1H, ArH), 7.84 (d, J = 8.4 Hz, 2H, ArH), 7.78-7.74 (m, 3H, ArH), 7.46 (s, 1H, ArH), 7.15 (d, J = 7.9 Hz, 1H, ArH), 6.93-6.89 (m, 2H, ArH), 6.73 (d, J = 8.1 Hz, 1H, ArH), 6.55 (t, J = 7.6 Hz, 1H, ArH), 5.87 (d, J = 6.0 Hz, 1H, ArH), 4.87 (s, 2H, $ArNH_2$), 4.07 (s, 3H, NCH_3), 4.05 (d, J = 5.4 Hz, 2H, NCH_2CO), 3.50 (s, 3H, NCH_3), 2.64 (s, 3H, $ArCH_3$).^{13}C NMR (100 MHz, DMSO) δ 168.61, 166.93, 162.89, 159.61, 156.26, 147.46, 144.53, 142.97, 142.36, 132.63, 128.43, 126.65, 126.28, 126.10, 123.32 122.21, 120.18, 119.96, 117.74, 116.44, 116.01, 114.44, 97.39, 43.68, 38.43, 37.85, 9.90.

HRMS (AP-ESI) m/z calcd for $C_{29}H_{29}N_9O_2$ $[M+H]^+$ 536.2444, found 536.2498. Retention time: 14.5 min, eluted with 55% methanol/45% water.

***N*-(3-((2-Aminophenyl)amino)-3-oxopropyl)-4-((4-((2,3-dimethyl-2*H*-indazol-6-yl)(methyl)amino) pyrimidin-2-yl)amino)benzamide (14b)**. White solid. 38% yield. Mp: 217-219 ℃. ^{1}H NMR (400 MHz, DMSO-d_6) δ 9.44 (s, 1H, ArNHAr), 9.16 (s, 1H, ArNHCO), 8.35 (t, J = 5.6 Hz, 1H, NH), 7.89 (d, J = 6.0 Hz, 1H, ArH), 7.82 (d, J = 8.8 Hz, 2H, ArH), 7.77 (dd, J = 0.8, 8.7 Hz, 1H, ArH), 7.70 (d, J = 8.6 Hz, 2H, ArH), 7.46 (dd, J = 0.8, 1.8 Hz, 1H, ArH), 7.15 (dd, J = 1.5, 7.8 Hz, 1H, ArH), 6.91-6.87 (m, 2H, ArH), 6.71 (dd, J = 1.4, 8.0 Hz, 1H, ArH), 6.53 (td, J = 1.5, 7.5 Hz, 1H, ArH), 5.84 (d, J = 6.0 Hz, 1H, ArH), 4.86 (s, 2H, $ArNH_2$), 4.06 (s, 3H, NCH_3), 3.55 (q, J = 6.6 Hz, 2H, NCH_2), 3.49 (s, 3H, NCH_3), 2.63-2.59 (m, 5H, $ArCH_3$ and CH_2CO). ^{13}C NMR (100 MHz, DMSO-d_6) δ 170.02, 166.53, 162.88, 159.67, 156.27, 147.46, 144.32, 142.64, 142.36, 132.63, 128.19, 126.64, 126.33, 126.07, 123.71, 122.21, 120.17, 119.96, 117.75, 116.47, 116.20, 114.43, 97.36, 38.42, 37.85, 36.53, 36.50, 9.90. HRMS (AP-ESI) m/z calcd for $C_{30}H_{31}N_9O_2$ $[M+H]^+$ 550.2679, found 550.2670. Retention time: 12.5 min, eluted with 58% methanol/42% water.

***N*-(4-((2-Aminophenyl)amino)-4-oxobutyl)-4-((4-((2,3-dimethyl-2*H*-indazol-6-yl)(methyl)amino) pyrimidin-2-yl)amino)benzamide (14c)**. White solid. 48% yield. Mp:150-152 ℃. ^{1}H NMR (400 MHz, DMSO-d_6) δ 9.44 (s, 1H, ArNHAr), 9.13 (s, 1H, ArNHCO), 8.29 (t, J = 5.6 Hz, 1H, NH), 7.89 (d, J = 6.0 Hz, 1H, ArH), 7.82 (d, J = 8.5 Hz, 2H, ArH), 7.77 (d, J = 8.7 Hz, 1H, ArH), 7.72 (d, J = 8.5 Hz, 2H, ArH), 7.46 (d, J = 1.7 Hz, 1H, ArH), 7.16 (dd, J = 1.5, 7.8 Hz, 1H, ArH), 6.91-6.87(m, 2H, ArH), 6.71 (dd, J = 1.4, 8.0 Hz, 1H, ArH), 6.53 (td, J = 1.5, 7.6 Hz, 1H, ArH), 5.84 (d, J = 6.0 Hz, 1H, ArH), 4.87 (s, 2H, $ArNH_2$), 4.06 (s, 3H, NCH_3), 3.50 (s, 3H, NCH_3), 3.32-3.19 (m, 2H, NCH_2), 2.63 (s, 3H, $ArCH_3$), 2.38 (t, J = 7.4 Hz, 2H, CH_2CO), 1.89-1.81 (m, 2H, CH_2). ^{13}C NMR (100

MHz, DMSO-*d6*) δ 171.37, 166.48, 162.88, 159.67, 156.29, 147.46, 144.26, 142.50, 142.37, 132.62, 128.20, 126.75, 126.19, 125.91, 123.92, 122.20, 120.18, 119.96, 117.74, 116.52, 116.23, 114.42, 97.32, 39.15, 38.42, 37.84, 33.79, 26.04, 9.90. HRMS (AP-ESI) m/z calcd for $C_{31}H_{33}N_9O_2$ $[M+H]^+$ 564.2835, found 564.2817. Retention time: 15.3 min, eluted with 65% methanol/35% water.

***N*-(5-((2-Aminophenyl)amino)-5-oxopentyl)-4-((4-((2,3-dimethyl-2*H*-indazol-6-yl)(methyl)amino) pyrimidin-2-yl)amino)benzamide (14d)**. White solid. 41% yield. Mp: 190-192 ℃. ^{1}H NMR (400 MHz, DMSO-d_6) δ 9.44 (s, 1H, ArNHAr), 9.10 (s, 1H, ArNHCO), 8.25 (t, J = 5.5 Hz, 1H, NH), 7.88 (d, J = 6.0 Hz, 1H, ArH), 7.81 (d, J = 8.5 Hz, 2H, ArH), 7.77 (d, J = 8.8 Hz, 1H, ArH), 7.69 (d, J = 8.5 Hz, 2H, ArH), 7.46 (d, J = 1.7 Hz, 1H, ArH), 7.16 (dd, J = 1.5, 7.8 Hz, 1H, ArH), 6.91-6.86 (m, 2H, ArH), 6.71 (dd, J = 1.5, 8.0 Hz, 1H, ArH), 6.53 (td, J = 1.4, 7.5 Hz, 1H, ArH), 5.84 (d, J = 6.0 Hz, 1H, ArH), 4.83 (s, 2H, $ArNH_2$), 4.06 (s, 3H, NCH_3), 3.49 (s, 3H, NCH_3), 3.31-3.22 (m, 2H, NCH_2), 2.63 (s, 3H, $ArCH_3$), 2.35 (t, J = 7.3 Hz, 2H, CH_2CO), 1.70-1.49 (m, 4H, CH_2). ^{13}C NMR (100 MHz, DMSO-d_6) δ 171.53, 166.31, 162.87, 159.67, 156.29, 147.45, 144.21, 142.36, 142.33, 132.63, 128.15, 126.82, 126.13, 125.73, 124.01, 122.20, 120.19, 119.95, 117.73, 116.59, 116.31, 114.42, 97.31, 39.66, 38.42, 37.84, 35.98, 29.46, 23.40, 9.90. HRMS (AP-ESI) m/z calcd for $C_{32}H_{35}N_9O_2$ $[M+H]^+$ 578.2992, found 578.2998. Retention time: 13.0 min, eluted with 67% methanol/33% water.

***N*-(6-((2-Aminophenyl)amino)-6-oxohexyl)-4-((4-((2,3-dimethyl-2*H*-indazol-6-yl)(methyl)amino) pyrimidin-2-yl)amino)benzamide (14e)**. White solid. 47% yield. Mp: 220-222 ℃. ^{1}H NMR (400 MHz, DMSO-d_6) δ 9.43 (s, 1H, ArNHAr), 9.09 (s, 1H, ArNHCO), 8.22 (t, J = 5.7 Hz, 1H, NH), 7.89 (d, J = 6.0 Hz, 1H, ArH), 7.81 (d, J = 8.5 Hz, 2H, ArH), 7.77 (d, J = 8.7 Hz, 1H, ArH), 7.69 (d, J = 8.5 Hz, 2H, ArH), 7.46 (d, J = 1.6 Hz, 1H, ArH), 7.15 (dd, J = 1.5, 7.8 Hz, 1H, ArH), 6.95-6.84 (m, 2H, ArH), 6.71 (dd, J = 1.5, 8.0 Hz, 1H, ArH), 6.52 (td, J = 1.5, 7.6 Hz, 1H, ArH), 5.84 (d, J =

6.0 Hz, 1H, ArH), 4.81 (s, 2H, $ArNH_2$), 4.07 (s, 3H, NCH_3), 3.49 (s, 3H, NCH_3), 3.25 (q, *J* = 6.6 Hz, 2H, NCH_2), 2.64 (s, 3H, $ArCH_3$), 2.33 (t, *J* = 7.4 Hz, 2H, CH_2CO), 1.67-1.52 (m, 4H, CH_2), 1.43-1.28 (m, 2H, CH_2). ^{13}C NMR (100 MHz, DMSO-d_6) δ 171.58, 166.28, 162.88, 159.68, 156.28, 147.46, 144.18, 142.36, 142.34, 132.62, 128.13, 126.87, 126.12, 125.75, 124.04, 122.20, 120.18, 119.96, 117.75, 116.62, 116.33, 114.42, 97.32, 39.47, 38.42, 37.85, 36.24, 29.61, 26.71, 25.61, 9.90. HRMS (AP-ESI) m/z calcd for $C_{33}H_{37}N_9O_2$ $[M+H]^+$592.3148, found 592.3136. Retention time: 14.8 min, eluted with 67% methanol/33% water.

***N*-(7-((2-Aminophenyl)amino)-7-oxoheptyl)-4-((4-((2,3-dimethyl-2*H*-indazol-6-yl)(methyl)amino) pyrimidin-2-yl)amino)benzamide (14f)**. White solid. 44% yield. Mp: 135-137 ℃. ^1H NMR (400 MHz, DMSO-d_6) δ 9.44 (s, 1H, ArNHAr), 9.10 (s, 1H, ArNHCO), 8.21 (t, *J* = 5.7 Hz, 1H, NH), 7.88 (d, *J* = 6.0 Hz, 1H, ArH), 7.81 (d, *J* = 8.6 Hz, 2H, ArH), 7.77 (d, *J* = 8.8 Hz, 1H, ArH), 7.68 (d, *J* = 8.5 Hz, 2H, ArH), 7.46 (d, *J* = 2.3 Hz, 1H, ArH), 7.14 (dd, *J* = 1.5, 7.9 Hz, 1H, ArH), 6.91-6.86 (m, 2H, ArH), 6.71 (dd, *J* = 1.5, 8.0 Hz, 1H, ArH), 6.53 (td, *J* = 1.5, 7.6 Hz, 1H, ArH), 5.84 (d, *J* = 6.0 Hz, 1H, ArH), 4.81 (s, 2H, $ArNH_2$), 4.06 (s, 3H, NCH_3), 3.49 (s, 3H, NCH_3), 3.23 (q, *J* = 6.6 Hz, 2H, NCH_2), 2.64 (s, 3H, $ArCH_3$), 2.31 (t, *J* = 7.3 Hz, 2H, CH_2CO), 1.66-1.44 (m, 4H, CH_2), 1.43-1.28 (m, 4H, CH_2). ^{13}C NMR (100 MHz, DMSO-d_6) δ 171.61, 166.29, 162.95, 159.69, 156.28, 147.47, 144.18, 142.42, 142.34, 132.61, 128.12, 126.88, 126.12, 125.73, 124.07, 122.19, 120.18, 119.97, 117.75, 116.64, 116.36, 114.42, 97.32, 39.52, 38.42, 37.84, 36.28, 29.68, 28.97, 26.81, 25.78, 9.89. HRMS (AP-ESI) m/z calcd for $C_{34}H_{39}N_9O_2$ $[M+H]^+$ 606.3227, found 606.3290. Retention time: 14.2 min, eluted with 70% methanol/30% water.

***N*-(8-((2-Aminophenyl)amino)-8-oxooctyl)-4-((4-((2,3-dimethyl-2*H*-indazol-6-yl)(methyl)amino) pyrimidin-2-yl)amino)benzamide (14g)**. White solid. 46% yield. Mp: 148-150 ℃. ^1H NMR (400

MHz, DMSO-d_6) ^{1}H NMR (400 MHz, DMSO-d_6) δ 9.42 (s, 1H, ArNHAr), 9.08 (s, 1H, ArNHCO), 8.19 (t, J = 5.6 Hz, 1H, NH), 7.88 (d, J = 6.0 Hz, 1H, ArH), 7.80 (d, J = 8.5 Hz, 2H, ArH), 7.77 (d, J = 8.8 Hz, 1H, ArH), 7.68 (d, J = 8.5 Hz, 2H, ArH), 7.46 (d, J = 1.7 Hz, 1H, ArH), 7.14 (dd, J = 1.5, 7.8 Hz, 1H, ArH), 6.92-6.84 (m, 2H, ArH), 6.70 (dd, J = 1.5, 8.0 Hz, 1H, ArH), 6.53 (td, J = 1.5, 7.5 Hz, 1H, ArH), 5.84 (d, J = 6.0 Hz, 1H, ArH), 4.80 (s, 2H, $ArNH_2$), 4.07 (s, 3H, NCH_3), 3.49 (s, 3H, NCH_3), 3.23 (q, J = 6.7 Hz, 2H, NCH_2), 2.64 (s, 3H, $ArCH_3$), 2.31 (t, J = 7.5 Hz, 2H, CH_2CO), 1.65-1.43 (m, 4H, CH_2), 1.40-1.25 (m, 6H, CH_2). ^{13}C NMR (100 MHz, DMSO-d_6) δ 171.61, 166.27, 162.88, 159.68, 156.28, 147.46, 144.17, 142.37, 142.33, 132.61, 128.13, 126.88, 126.12, 125.72, 124.07, 122.20, 120.19, 119.96, 117.75, 116.64, 116.35, 114.42, 97.30, 39.45, 38.42, 37.84, 36.25, 29.76, 29.16, 29.09, 26.95, 25.77, 9.89. HRMS (AP-ESI) m/z calcd for $C_{35}H_{41}N_9O_2$ $[M+H]^+$ 620.3461, found 620.3449. Retention time: 17.4 min, eluted with 70% methanol/30% water.

In Vitro HDAC Inhibition Fluorescence Assay. In vitro HDACs inhibition assays were conducted as previously described.[41] In brief, 10 μL of enzyme solution (HeLa cell nuclear extract, HDAC2, HDAC6 or HDAC8) was mixed with different concentrations of tested compound (50 μL). The mixture was incubated at 37℃ for 5 mins, followed by adding 40 μL fluorogenic substrate (Boc-Lys(acetyl)-AMC for HeLa cell nuclear extracts, HDAC2 and HDAC6, Boc-Lys(triflouroacetyl)-AMC for HDAC8). After incubation at 37℃ for 30 mins, the mixture was quenched by addition of 100 μL of developer containing trypsin and Trichostatin A (TSA). Over another incubation at 37 ℃ for 20 min, fluorescence intensity was measured using a microplate reader at excitation and emission wavelengths of 390 and 460 nm, respectively. The inhibition ratios were calculated from the fluorescence intensity readings of tested wells relative to those of control wells, and the IC_{50} values were calculated using a regression analysis of the concentration/inhibition data.

Kinase Inhibition Assay. The kinase (VEGFR-1, -2, -3, PDGFRβ, FGFR-1, C-Kit and C-Fms) inhibitory activity was measured by HUAWEI PHARMA (Ji' nan, China) with the Kinase-Glo^{TM} Luminescent Kinase Assay. Briefly, the tested compounds, kinase, substrate, and ATP were diluted in kinase buffer to the indicated concentrations, covered the assay plate, and incubated at room temperature for 40 min. Then the Kinase-Glo reagent was added and incubated for an additional 15 min. At the end point, the luminescence was recorded on a microplate reader (SpectraMax M5). The IC_{50} values were calculated using nonlinear regression with normalized dose−response fit using Prism GraphPad software.

Docking Study. The crystal structures of VEGFR-2 (PDB code: 3CJG), HDAC2 (PDB code: 5IWG) and HDAC6 (PDB code: 5EEI) were obtained from Protein Data Bank. Water molecules and co-crystallized ligands were removed from the proteins using Sybyl X_2.1. Compounds were prepared using Sketch and optimized with Tripos force field. Surflex-Dock Geom (SFXC) was used to dock compounds into the binding site of the three enzymes. For HDAC2 and HDAC6, the protomol was defined as 10Å radius around Zinc ion. For VEGFR-2, the protomol was generated based on the ligand in the crystal structure. Other parameters were set as default values.

Cell Proliferation Inhibition Assay. All cell lines were maintained in RPMI1640 medium containing 10% FBS at 37 ℃ in a 5% CO_2 humidified incubator. Cell proliferation assay was determined by the MTT (3-[4,5-Dimethyl-2-thiazolyl]-2,5-diphenyl-2h-tetrazolium bromide) method. Briefly, cells were passaged the day before dosing into a 96-well plate, allowed to grow for 12 h, and then treated with different concentrations of compound for 72 h. A 0.5% MTT solution was added to each well. After incubation for another 4 h, formazan formed from MTT was extracted by adding 200 μL of DMSO. Absorbance was then determined using an ELISA reader at 570 nm.

Western Blotting Assay. The HeLa or HUVEC cells were treated with compounds or DMSO for a

specified period of time. Then the cells were washed twice with cold PBS and lysed in ice-cold RIPA buffer. Lysates were cleared by centrifugation. Protein concentrations were determined using the BCA assay. Equal amounts of cell extracts were then resolved by SDS-PAGE, transferred to nitrocellulose membranes and probed with ac-histone H4 antibody, ac-tubulin antibody, β-actin antibody, phosphorylated VEGFR-2 antibody and total VEGFR-2 antibody, respectively. Blots were detected using an enhanced chemiluminescence system.

Tubular Structure Formation Assay in HUVECs. HUVEC tuber formation assay was established as previously described.[42] Matrigel (100 μL; BD biosciences, NJ) was added into test well of 96-well plates and then allowed to polymerize for 0.5 h at 37 °C. HUVECs were trypsinized and seeded at the density of 40000 per well in M199 (5% FBS) containing DMSO or test compounds for 6 h at 37 °C in a CO_2 incubator. The morphological changes of the cells and tubes formation were observed under a phase-contrast microscope (OLYMPUS IX51) and photographed at a 200 magnification. Experiments were repeated three times.

Ex Vivo Antiangiogenic Assay in Rat Aortic Ring. Rat thoracic aorta rings (TARs) assay was established as previously described.[42] Matrigel (100 μL; BD biosciences, NJ) was added into test well of 96-well plates and then allowed to polymerize for 0.5 h at 37 °C. Sprague–Dawley rats of 4 to 6-week-old were sacrificed and aortas were harvested. Each aorta was cut into 1-mm slices and embedded in additional 100 μL of Matrigel in 96-well plates. After that, the rings were incubated for 30 min at 37 °C and 5% CO_2. Aorta rings were treated with the vehicle (0.5% DMSO) or compounds each day for 6 days and photographed on the 7th day at ×200 magnification. Experiments were repeated three times.

Pharmacokinetic Study. All experiments involving laboratory animals were performed with the approval of the Shandong University Laboratory Animal Center ethics committee. Compound **6d**

(hydrochlorate) was subjected to PK studies in SD rats. Compound **6d** (hydrochlorate) was administrated via the oral route at 10 mg/kg or administrated via the intravenous route at 2 mg/kg. Blood samples were collected from each animal via jugular vein and stored in ice (0-4 °C) at the specific time points. Plasma was separated from the blood by centrifugation and stored in a freezer at −80 °C. All samples for the tested compounds were analyzed by LC-MS/MS.

Efficacy Study in Human Cancer Xenograft Model. In vivo human tumor xenograft models were established as previously described.[41] 1×10^7 human colorectal adenocarcinoma cells (HT-29) were inoculated subcutaneously in the right flank of male BALB/c-nu mice (5-6 weeks old, Beijing HFK Bioscience Co., Ltd.). Ten days after injection, tumors were palpable and mice were randomized into treatment and control groups (6 mice per group). The treatment groups received specified concentrations of compounds by oral administration, and the blank control group received oral administration of equal volume of PBS (5% DMSO). During treatment, subcutaneous tumors were measured with vernier caliper every three days, and body weight was monitored regularly. Tumor volume (V) was estimated using the equation ($V = ab^2 / 2$, where a and b stand for the longest and shortest diameter, respectively). T/C was calculated according to the following formula:

T/C = the mean RTV of treated group / the mean RTV of control group.

RTV, namely relative tumor volume = V_t / V_0, (V_t: the tumor volume measured at the end of treatment; V_0: the tumor volume measured at the beginning of treatment)

After treatment, mice were sacrificed and dissected to weigh the tumor tissues and to examine the internal organ injury by macroscopic analysis. TGI was calculated according to the following formula:

TGI = (the mean tumor weight of control group – the mean tumor weight of treated group) / the mean tumor weight of control group.

All the obtained data were used to evaluate the antitumor potency and toxicity of compounds. Data were analyzed by Student's two-tailed t test. A P level < 0.05 was considered statistically significant.

ASSOCIATED CONTENT

Supporting information

In vitro cytotoxic activities of selected compounds against HUVECs, ^{1}H NMR and ^{13}C NMR spectra of all target compounds;

Molecular formula stings (CSV)

AUTHOR INFORMATION

Corresponding Author

*Y. Z.: phone, +86 531 88382009; E-mail: zhangyingjie@sdu.edu.cn

ORCID

Yingjie Zhang: 0000-0001-6118-6695

Author Contributions

The manuscript was written through contributions of all authors who gave approval to the final version of the manuscript.

Notes

The authors declare no competing financial interest.

ACKNOWLEGEMENTS

This work was supported by National High-Tech R&D Program of China (863 Program) (2014AA020523), National Natural Science Foundation of China (21302111), Natural Science Foundation of Shandong Province (Grant No. ZR201709190013), Major Project of Science and Technology of Shandong Province (2015ZDJS04001, 2017CXGC1401), Young Scholars Program of Shandong University (YSPSDU, 2016WLJH33).

ABBREVIATIONS USED

DMF, *N*,*N*-dimethylformamide; EtOAc, ethyl acetate; HDAC, histone deacetylase; HPLC, high performance liquid chromatography; HUVECs, human umbilical vein endothelial cells; IC_{50}, half-maximum inhibitory concentration; MeOH, methanol; MTT, 3-(4,5-dimethylthizaol-2-yl)-2,5-diphenyltetrazolium bromide; NMR, nuclear magnetic resonance; rt, room temperature; TEA, trimethylamine; THF, tetrahydrofuran; TBTU, O-(Benzotriazol-1-yl)-N,N,N',N'-tetramethyluronium tetrafluoroborate; VEGFR-2, vascular endothelial growth receptor-2; ZBG, zinc binding group;

REFERENCES

(1). Sawyers, C. Targeted cancer therapy. *Nature* **2004**, *432*, 294.

(2). Hanahan, D.; Weinberg, R. A. Hallmarks of cancer: the next generation. *Cell* **2011**, *144*, 646-674.

(3). Hanahan, D.; Weinberg, R. A. The hallmarks of cancer. *Cell* **2000**, *100*, 57-70.

(4). Anighoro, A.; Bajorath, J.; Rastelli, G. Polypharmacology: challenges and opportunities in drug discovery: miniperspective. *J. Med. Chem.* **2014**, *57*, 7874-7887.

(5). Peters, J.-U. Polypharmacology–foe or friend? *J. Med. Chem.* **2013**, *56*, 8955-8971.

(6). Morphy, R.; Rankovic, Z. Designed multiple ligands. an emerging drug discovery paradigm. *J. Med. Chem.* **2005**, *48*, 6523-6543.

(7). M O'Boyle, N.; J Meegan, M. Designed multiple ligands for cancer therapy. *Curr. Med. Chem.* **2011**, *18*, 4722-4737.

(8). Jones, P. A.; Issa, J.-P. J.; Baylin, S. Targeting the cancer epigenome for therapy. *Nat. Rev. Genet.* **2016**, *17*, 630-641.

(9). Kelly, T. K.; De Carvalho, D. D.; Jones, P. A. Epigenetic modifications as therapeutic targets. *Nat. Biotechnol.* **2010**, *28*, 1069-1078.

(10). Zwergel, C.; Stazi, G.; Valente, S.; Mai, A. Histone deacetylase inhibitors: updated studies in various epigenetic-related diseases. *J. Clin. Epigenetics* **2016**, *2*, 1-15.

(11). Falkenberg, K. J.; Johnstone, R. W. Histone deacetylases and their inhibitors in cancer, neurological diseases and immune disorders. *Nat. Rev. Drug Discov.* **2014**, *13*, 673-691.

(12). Zagni, C.; Floresta, G.; Monciino, G.; Rescifina, A. The search for potent, small-molecule HDACIs in cancer treatment: a decade after Vorinostat. *Med. Res. Rev.* **2017**, *37*, 1373-1428.

(13). Guha, M. HDAC inhibitors still need a home run, despite recent approval. *Nat. Rev. Drug Discov.* **2015**, *14*, 225-226.

(14). Choy, E.; Flamand, Y.; Balasubramanian, S.; Butrynski, J. E.; Harmon, D. C.; George, S.; Cote, G. M.; Wagner, A. J.; Morgan, J. A.; Sirisawad, M. Phase 1 study of oral abexinostat, a histone deacetylase inhibitor, in combination with doxorubicin in patients with metastatic sarcoma. *Cancer* **2015**, *121*, 1223-1230.

(15). Whittle, J. R.; Desai, J. Histone deacetylase inhibitors in cancer: what have we learned? *Cancer* **2015**, *121*, 1164-1167.

(16). Verbrugge, I.; Johnstone, R. W.; Bots, M. Promises and challenges of anticancer drugs that target the epigenome. *Epigenomics* **2011**, *3*, 547-565.

(17). Dong, G.; Chen, W.; Wang, X.; Yang, X.; Xu, T.; Wang, P.; Zhang, W.; Rao, Y.; Miao, C.; Sheng, C. Small molecule inhibitors simultaneously targeting cancer metabolism and epigenetics: discovery of novel nicotinamide phosphoribosyltransferase (NAMPT) and histone deacetylase (HDAC) dual inhibitors. *J. Med. Chem.* **2017**, *60*, 7965-7983.

(18). Yao, L.; Mustafa, N.; Tan, E. C.; Poulsen, A.; Singh, P.; Duong-Thi, M.-D.; Lee, J. X.; Ramanujulu, P. M.; Chng, W. J.; Yen, J. J. Design and synthesis of ligand efficient dual inhibitors of janus kinase (JAK) and histone deacetylase (HDAC) based on Ruxolitinib and Vorinostat. *J. Med. Chem.* **2017**, *60*, 8336-8357.

(19). Yang, E. G.; Mustafa, N.; Tan, E. C.; Poulsen, A.; Ramanujulu, P. M.; Chng, W. J.; Yen, J. J.; Dymock, B. W. Design and synthesis of janus kinase 2 (JAK2) and histone deacetlyase (HDAC) bispecific inhibitors based on pacritinib and evidence of dual pathway inhibition in hematological cell lines. *J. Med. Chem.* **2016**, *59*, 8233-8262.

(20). Liao, Y.; Niu, X.; Chen, B.; Edwards, H.; Xu, L.; Xie, C.; Lin, H.; Polin, L.; Taub, J. W.; Ge, Y. Synthesis

and antileukemic activities of piperlongumine and HDAC inhibitor hybrids against acute myeloid leukemia cells. *J. Med. Chem.* **2016**, *59*, 7974-7990.

(21). Ling, Y.; Xu, C.; Luo, L.; Cao, J.; Feng, J.; Xue, Y.; Zhu, Q.; Ju, C.; Li, F.; Zhang, Y. Novel β-carboline/hydroxamic acid hybrids targeting both histone deacetylase and DNA display high anticancer activity via regulation of the p53 signaling pathway. *J. Med. Chem.* **2015**, *58*, 9214-9227.

(22). Tang, C.; Li, C.; Zhang, S.; Hu, Z.; Wu, J.; Dong, C.; Huang, J.; Zhou, H.-B. Novel bioactive hybrid compound dual targeting estrogen receptor and histone deacetylase for the treatment of breast cancer. *J. Med. Chem.* **2015**, *58*, 4550-4572.

(23). Folkman, J. Tumor angiogenesis: therapeutic implications. *N. Engl. J. Med.* **1971**, *285*, 1182-1186.

(24). Brown, J. M.; Giaccia, A. J. The unique physiology of solid tumors: opportunities (and problems) for cancer therapy. *Cancer Res.* **1998**, *58*, 1408-1416.

(25). Musumeci, F.; Radi, M.; Brullo, C.; Schenone, S. Vascular endothelial growth factor (VEGF) receptors: drugs and new inhibitors. *J. Med. Chem.* **2012**, *55*, 10797-10822.

(26). Liang, X.; Xu, F.; Li, X.; Ma, C.; Zhang, Y.; Xu, W. VEGF signal system: the application of antiangiogenesis. *Curr. Med. Chem.* **2014**, *21*, 894-910.

(27). Ferrara, N.; Adamis, A. P. Ten years of anti-vascular endothelial growth factor therapy. *Nat. Rev. Drug Discov.* **2016**, *15*, 385-403.

(28). Harris, P. A.; Boloor, A.; Cheung, M.; Kumar, R.; Crosby, R. M.; Davis-Ward, R. G.; Epperly, A. H.; Hinkle, K. W.; Hunter III, R. N.; Johnson, J. H. Discovery of 5-[[4-[(2, 3-dimethyl-2 H-indazol-6-yl) methylamino]-2-pyrimidinyl] amino]-2-methyl-benzenesulfonamide (Pazopanib), a novel and potent vascular endothelial growth factor receptor inhibitor. *J. Med. Chem.* **2008**, *51*, 4632-4640.

(29). Brotelle, T.; Bay, J.-O. Pazopanib for treatment of renal cell carcinoma and soft tissue sarcomas. *Bull Cancer* **2014**, *101*, 641-646.

(30). Koinis, F.; Agelaki, S.; Karavassilis, V.; Kentepozidis, N.; Samantas, E.; Peroukidis, S.; Katsaounis, P.; Hartabilas, E.; Varthalitis, I.; Messaritakis, I. Second-line pazopanib in patients with relapsed and refractory

small-cell lung cancer: a multicentre phase II study of the hellenic oncology research group. *Br. J. Cancer* **2017**, *117*, 8-14.

(31). Choueiri, T. K.; Escudier, B.; Powles, T.; Mainwaring, P. N.; Rini, B. I.; Donskov, F.; Hammers, H.; Hutson, T. E.; Lee, J.-L.; Peltola, K. Cabozantinib versus everolimus in advanced renal-cell carcinoma. *N. Engl. J. Med.* **2015**, *373*, 1814-1823.

(32). Vyse, S.; McCarthy, F.; Broncel, M.; Paul, A.; Wong, J. P.; Bhamra, A.; Huang, P. H. Quantitative phosphoproteomic analysis of acquired cancer drug resistance to pazopanib and dasatinib. *J. Proteom.* **2018**, *170*, 130-140.

(33). Torok, S.; Rezeli, M.; Kelemen, O.; Vegvari, A.; Watanabe, K.; Sugihara, Y.; Tisza, A.; Marton, T.; Kovacs, I.; Tovari, J. Limited tumor tissue drug penetration contributes to primary resistance against angiogenesis inhibitors. *Theranostics* **2017**, *7*, 400-412.

(34). Chan, D.; Zheng, Y.; Tyner, J. W.; Chng, W. J.; Chien, W. W.; Gery, S.; Leong, G.; Braunstein, G. D.; Koeffler, H. P. Belinostat and panobinostat (HDACI): in vitro and in vivo studies in thyroid cancer. *J. Cancer Res. Clin. Oncol.* **2013**, *139*, 1507-1514.

(35). Tavallai, S.; Hamed, H. A.; Grant, S.; Poklepovic, A.; Dent, P. Pazopanib and HDAC inhibitors interact to kill sarcoma cells. *Cancer Biol. Ther.* **2014**, *15*, 578-585.

(36). Booth, L.; Roberts, J. L.; Sander, C.; Lee, J.; Kirkwood, J. M.; Poklepovic, A.; Dent, P. The HDAC inhibitor AR42 interacts with pazopanib to kill trametinib/dabrafenib-resistant melanoma cells in vitro and in vivo. *Oncotarget* **2017**, *8*, 16367-16386.

(37). Fu, S.; Hou, M.; Naing, A.; Janku, F.; Hess, K.; Zinner, R.; Subbiah, V.; Hong, D.; Wheler, J.; Piha-Paul, S. Phase I study of pazopanib and vorinostat: a therapeutic approach for inhibiting mutant p53-mediated angiogenesis and facilitating mutant p53 degradation. *Ann. Oncol.* **2015**, *26*, 1012-1018.

(38). Aggarwal, R.; Thomas, S.; Pawlowska, N.; Bartelink, I.; Grabowsky, J.; Jahan, T.; Cripps, A.; Harb, A.; Leng, J.; Reinert, A. Inhibiting histone deacetylase as a means to reverse resistance to angiogenesis inhibitors: phase I study of abexinostat plus pazopanib in advanced solid tumor malignancies. *J. Clin. Oncol.* **2017**, *35*,

1231-1239.

(39). Miller, T. A.; Witter, D. J.; Belvedere, S. Histone deacetylase inhibitors. *J. Med. Chem.* **2003**, *46*, 5097-5116.

(40). Hermant, P.; Bosc, D.; Piveteau, C.; Gealageas, R.; Lam, B.; Ronco, C.; Roignant, M.; Tolojanahary, H.; Jean, L.; Renard, P.-Y. Controlling plasma stability of hydroxamic acids: a medchem toolbox. *J. Med. Chem.* **2017**, *60*, 9067-9089.

(41). Li, X.; Inks, E. S.; Li, X.; Hou, J.; Chou, C. J.; Zhang, J.; Jiang, Y.; Zhang, Y.; Xu, W. Discovery of the first N-hydroxycinnamamide-based histone deacetylase 1/3 dual inhibitors with potent oral antitumor activity. *J. Med. Chem.* **2014**, *57*, 3324-3341.

(42). Xu, F.; Jia, Y.; Wen, Q.; Wang, X.; Zhang, L.; Zhang, Y.; Xu, W. Synthesis and biological evaluation of N-(4-hydroxy-3-mercaptonaphthalen-1-yl) amides as inhibitors of angiogenesis and tumor growth. *Eur. J. Med. Chem.* **2013**, *64*, 377-388.

Table of Contents Graphic

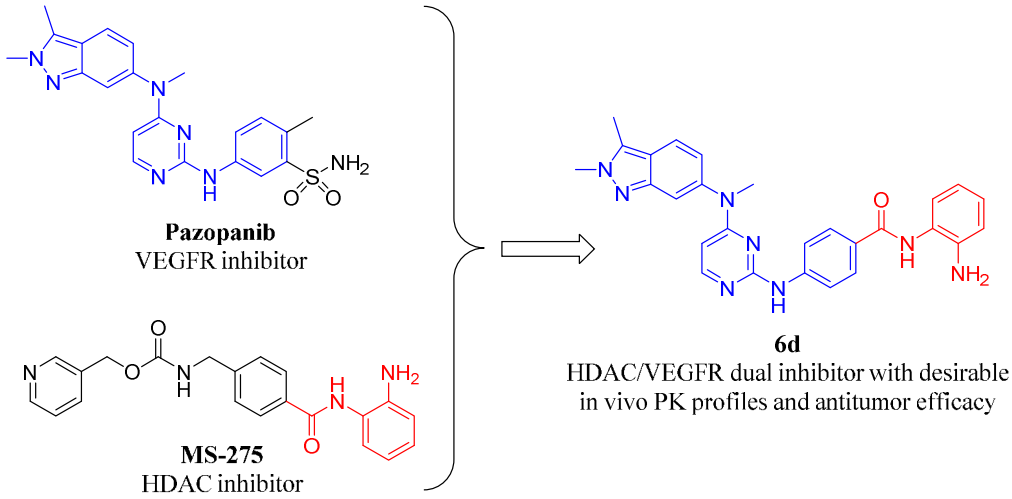
Pazopanib
VEGFR inhibitor
MS-275
HDAC inhibitor
6d
HDAC/VEGFR dual inhibitor with desirable
in vivo PK profiles and antitumor efficacy